RESEARCH ARTICLE

WILEY · JCN RESEARCH IN SYSTEMS NEUROSCIENCE · THE JOURNAL OF COMPARATIVE NEUROLOGY

Mapping the distribution of language related genes *FoxP1*, *FoxP2*, and *CntnaP2* in the brains of vocal learning bat species

Pedro M. Rodenas-Cuadrado[1] | Janine Mengede[1] | Laura Baas[1] |

Paolo Devanna[1] | Tobias A. Schmid[2] | Michael Yartsev[2,3] | Uwe Firzlaff[4] |

Sonja C. Vernes[1,5] (iD)

[1]Neurogenetics of Vocal Communication Group, Max Planck Institute for Psycholinguistics, Nijmegen 6500 AH, The Netherlands

[2]Helen Wills Neuroscience Institute, UC Berkeley, Berkeley, California 94720

[3]Department of Bioengineering, UC Berkeley, 306 University of California, Berkeley, California 94720

[4]Department Tierwissenschaften, Lehrstuhl für Zoologie, TU München, München 85354, Germany

[5]Donders Centre for Cognitive Neuroimaging, Nijmegen 6525 EN, The Netherlands

Correspondence
Sonja C. Vernes, Neurogenetics of Vocal Communication Group, Max Planck Institute for Psycholinguistics, Nijmegen, 6500 AH, The Netherlands.
Email: Sonja.Vernes@mpi.nl

Funding information
Marie Curie Career Integration Grant, Grant/Award Number: PCIG12-GA-2012-333978; Max Planck Research Group Grant; Human Frontiers Science Program (HFSP) Research grant, Grant/Award Number: RGP0058/2016

Abstract

Genes including *FOXP2*, *FOXP1*, and *CNTNAP2*, have been implicated in human speech and language phenotypes, pointing to a role in the development of normal language-related circuitry in the brain. Although speech and language are unique to humans a comparative approach is possible by addressing language-relevant traits in animal systems. One such trait, vocal learning, represents an essential component of human spoken language, and is shared by cetaceans, pinnipeds, elephants, some birds and bats. Given their vocal learning abilities, gregarious nature, and reliance on vocalizations for social communication and navigation, bats represent an intriguing mammalian system in which to explore language-relevant genes. We used immunohistochemistry to detail the distribution of FoxP2, FoxP1, and Cntnap2 proteins, accompanied by detailed cytoarchitectural histology in the brains of two vocal learning bat species; *Phyllostomus discolor* and *Rousettus aegyptiacus*. We show widespread expression of these genes, similar to what has been previously observed in other species, including humans. A striking difference was observed in the adult *P. discolor* bat, which showed low levels of FoxP2 expression in the cortex that contrasted with patterns found in rodents and nonhuman primates. We created an online, open-access database within which all data can be browsed, searched, and high resolution images viewed to single cell resolution. The data presented herein reveal regions of interest in the bat brain and provide new opportunities to address the role of these language-related genes in complex vocal-motor and vocal learning behaviors in a mammalian model system.

KEYWORDS
bats, CNTNAP2, FOXP1, FOXP2, language, vocal learning

Abbreviations: A, Amygdala; AAF, Anterior auditory field; AB, Accessory basal amygdaloid complex; ACC, Anterior Cingulate Cortex; AI, Primary auditory cortex; BLa, Basolateral amygdaloid nucleus, pars anterior; BLp, Basolateral amygdaloid nucleus, pars posterior; Bmg, Basal nucleus of the amygdala, magnocellular part; C, Caudate; Ce, Central amygdaloid nucleus; CL, Centrolateral nucleus; CM, Centromedial nucleus; Ctx, Cortex; DG, Dentate gyrus; GL, Granular layer; GP, Globus Pallidus; Hi, Hippocampus; Hy, Hypothalamus; IA, Intercalated amygdaloid nucleus; IC, Inferior colliculus; IHC, Immunohistochemistry; IO, Inferior Olives; La, Lateral amygdaloid nucleus, pars anterior; LD, Laterodorsal nucleus; LGd, lateral Geniculate nucleus, dorsal; LGv, lateral Geniculate nucleus, ventral; lHb, lateral Habenular nucleus; Lp, Lateral amygdaloid nucleus, pars posterior; MD, Mediodorsal nucleus; Me, Medial amygdaloid nucleus; mHb, medial Habenular nucleus; ML, Molecular layer; P, Putamen; PC, Paracentral nucleus; PCL, Purkinje cell layer; PDF, Posterior dorsal field; PV, Paraventricular nucleus; Re, nucleus of Reuniens; Rh, Rhomboidal nucleus; RT, Reticular nucleus; SC, Superior colliculus; Th, Thalamus; VA, Ventral anterior nucleus; VL, Ventrolateral nucleus; VM, Ventromedial nucleus; vMGN, ventral Medial geniculate nucleus; VPL, Ventroposterolateral nucleus.

1 | INTRODUCTION

How language evolved and is encoded in our biology represents one of the most challenging problems in the quest to understand what makes us human. Although language is unique to humans, we can address this topic using a comparative approach by studying language-relevant traits shared with other animals. Vocal production learning (VPL), the ability to learn to modify vocal outputs in response to auditory feedback, is a key skill employed by humans to facilitate spoken language (Janik & Slater, 2000; Petkov & Jarvis, 2012). Although VPL is a rare trait, it has been demonstrated in some birds, cetaceans, pinnipeds, elephants and some bats (Janik & Slater,

1997; Petkov & Jarvis, 2012; Knornschild, 2014). As has been shown by elegant work in songbirds, studying VPL in animal models can shed light on the neurobiological and genetic mechanisms underlying this trait (Doupe & Kuhl, 1999; Mello, 2002; Goldstein, King, & West, 2003; Doupe, Solis, Kimpo, & Boettiger, 2004; Jarvis, 2004; Scharff & White, 2004; Doupe, Perkel, Reiner, & Stern, 2005; White, Fisher, Geschwind, Scharff, & Holy, 2006; Haesler et al., 2007; Bolhuis, Oka-noya, & Scharff, 2010; Hilliard, Miller, Fraley, Horvath, & White, 2012; Petkov & Jarvis, 2012; Brainard & Doupe, 2013). To date, little is known about the neurogenetic mechanisms underlying VPL in mammalian vocal learners—partly due to difficulties performing such studies on large animals like sea mammals or elephants.
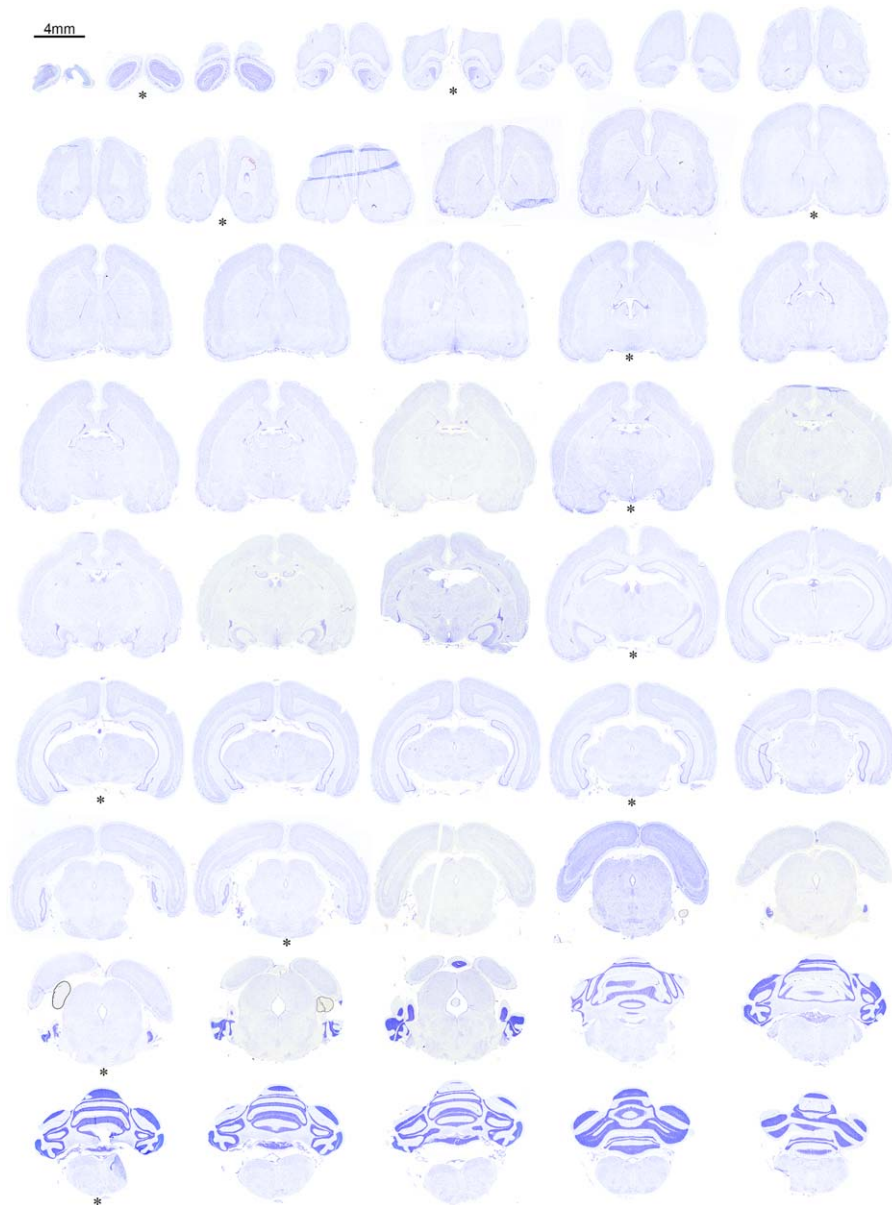

FIGURE 1 Histological sections displaying the cytoarchitecture of the *P. discolor* bat brain. The collection of 49 coronal plane sections of the *P. discolor* bat brain used for histology, arranged anterior to posterior. The 4 μm thick sections shown in this figure were Nissl stained to show the cytoarchitecture of the bat brain, and adjacent 4 μm sections were used for IHC (shown in subsequent figures) to determine the expression patterns of FoxP2, FoxP1, and Cntnap2. Representative tissue sections used for detailed analysis are indicated by an asterisk below the relevant brain slice. Scale bar represents 4 mm

However, bats are emerging as a promising mammalian system in which to address these questions given that a number of species display vocal learning abilities, their highly gregarious nature, and their amenability to lab based experiments (Knornschild, 2014; Vernes, 2017). Determining the expression patterns of genes implicated in speech and language in vocal learning bats will point to brain regions that may be important for vocal learning and allow detailed neurogenetic investigations of how these genes directly influence this complex vocal behavior. Herein we present an in-depth histological investigation of three key genes implicated in human speech and language phenotypes (*FoxP2*, *FoxP1*, and *CntnaP2*[1]) in the brains of two bat species with evidence of vocal learning; *Phyllostomus discolor* (*P. discolor*) and *Rousettus aegyptiacus* (*R. aegyptiacus*).

FOXP2 was the first and is the most well characterized gene known to be involved in human language (Lai, Fisher, Hurst, Vargha-Khadem, & Monaco, 2001; Fisher & Scharff, 2009). *FOXP2* mutations were identified as a monogenic cause of speech and language disorder in an extended pedigree (known as the "KE family") and has since been found in numerous similarly affected but unrelated individuals (Morgan, Fisher, Scheffer, & Hildebrand, 2016). The *FOXP1* gene is closely related to *FOXP2* and mutations in this gene have also been found in children with language impairments, although unlike individuals with *FOXP2* mutations, these children usually display additional deficits including autism spectrum disorder, mild to moderate intellectual disabilities and motor impairments (Hamdan et al., 2010; Lozano, Vino, Lozano, Fisher, & Deriziotis, 2015; Sollis et al., 2016). Both FOXP2 and FOXP1 are members of the same protein family that act to regulate the expression of other genes in the genome, determining when and where they are switched on or off (Li, Weidenfeld, & Morrisey, 2004). One of the genes regulated by FOXP2 is *CNTNAP2*, and this gene has itself been directly associated with specific language impairment in children (Vernes et al., 2008). *CNTNAP2* encodes a transmembrane protein (known as Caspr2) that facilitates clustering of proteins in specific regions of myelinated axons and at synapses (Rodenas-Cuadrado, Ho, & Vernes, 2014). Mutations in *CNTNAP2* can produce a range of phenotypes in addition to speech and language problems including autistic phenotypes, intellectual disability, and epilepsy (Strauss et al., 2006; Alarcón et al., 2008; Bakkaloglu et al., 2008; Rodenas-Cuadrado et al., 2014; Rodenas-Cuadrado et al., 2016). In a vocal learning avian species (zebra finch), *FoxP2*, *FoxP1*, and *CntnaP2* are all expressed in key regions of the song learning circuitry, with enrichment across different combinations of nuclei for each gene (Teramitsu, 2004, 2006; Panaitof, Abrahams, Dong, Geschwind, & White, 2010; Tanimoto, Teramitsu, Poopatanapong, Torrisi, & White, 2010; Condro & White, 2014). These genes have also been explored in the developing human brain, and in primate and rodent models, displaying widespread expression across circuitry that contribute to vocal-motor perception and production (Ferland, Cherry, Preware, Morrisey, & Walsh, 2003; Lai, Gerrelli,

---

[1]Uppercase denotes the human gene, lowercase denotes mouse and mixed upper and lower is used for all other species, according to standard nomenclature. Italics are used when referring to genes and standard text is used for proteins.

FIGURE 2 Histological sections displaying the cytoarchitecture of the *R. aegyptiacus* bat brain. The collection of 45 coronal plane sections (single hemisphere) of the *R. aegyptiacus* bat brain used for histology, arranged anterior to posterior. The 4 μm thick sections shown in this figure were Nissl stained to show the cytoarchitecture of the brain, and adjacent 4 μm sections were used for IHC (shown in main figures) to determine the expression patterns of FoxP2, FoxP1, and Cntnap2. Representative tissue sections used for detailed analysis are indicated by an asterisk below the relevant section. Scale bar represents 4 mm

Monaco, Fisher, & Copp, 2003; Haesler et al., 2004; Teramitsu, 2004; Alarcón et al., 2008; Campbell, Reep, Stoll, Ophir, & Phelps, 2009; Panaitof et al., 2010; Condro & White, 2014; Gordon et al., 2016). As such, expression of these three genes is expected to be found in

circuits subserving vocal-motor and/or vocal-learning pathways in bat brains.

Evidence of vocal learning has been described in bats across three different families; Phyllostomidae, Pteropodidae, and Emballonuridae (Knornschild, 2014; Prat, Taub, & Yovel, 2015), and a few other bats show promise as vocal learners (Knornschild, 2014). *P. discolor* of the Phyllostomidae family was the first bat species suggested to be a vocal learner when it was shown that pups of this species modify their calls in response to the maternal calls to which they are exposed (Esser & Schmidt, 1989; Esser, 1994). *R. aegyptiacus* of the Pteropodidae family is also thought to be a vocal learner, since juveniles require vocal input from adults in order to learn the appropriate adult vocal repertoire. Features of their learned vocalizations can also be modified using auditory playback, suggestive that auditory input in this species is both necessary and sufficient for acquiring vocalizations (Prat et al., 2015). For both species the learned calls are relatively low frequency calls (in the range of ~10–60 kHz) that are laryngeally produced and used for social communication (Esser & Schmidt, 1990; Prat et al., 2015). Both species are capable of echolocation, however the mechanisms employed are different; *P. discolor* uses frequency modulated echolocation calls generated from the larynx to navigate (Esser & Kiefer, 1996), while *R. aegyptiacus* is not capable of laryngeal echolocation, but uses tongue clicking to facilitate sonar navigation (Yovel, Geva-Sagiv, & Ulanovsky, 2011). In addition to the evidence for vocal learning, *P. discolor* and *R. aegyptiacus* display a number of other advantages recommending them for study; unlike many bat species, *P. discolor* and *R. aegyptiacus* can be maintained in captive breeding colonies facilitating controlled study of the neurogenetic bases of traits like vocal learning. Furthermore, these two bat species are positioned at either end of the chiropteran phylogenetic tree (Teeling et al., 2005) making comparative study of these species likely to reveal generalizable features of vocal learning.

Herein, we report detailed expression patterns for the FoxP2, FoxP1, and CntnaP2 (Caspr2) proteins, accompanied by cytoarchitectural histology, throughout the brains of *P. discolor* and *R. aegyptiacus* bats. All high-resolution images have been made available via a searchable database, providing an open access histological and neurogenetic resource. Our data reveal distributed expression of these key language-related genes and highlights brain regions where these genes may contribute to vocal communication and vocal learning in bats.

2 | MATERIALS AND METHODS

2.1 | Animal housing and conditions

Phyllostomus discolor bats originated from a breeding colony in the Department Biology II of the Ludwig-Maximilians-University in Munich. In this colony animals were kept under semi-natural conditions (12-hr day/12-hr night cycle, 65–70% relative humidity, 28°C) with free access to food and water. Approval to keep and breed the bats was issued by the Munich district veterinary office. Under German Law on Animal Protection a special ethical approval is not needed for this procedure, but the number of sacrificed animals was reported to the district veterinary office.

TABLE 1 Details of antibodies used for immunohistochemistry

Name	Product #	Lot #	Company	Raised in	Antigen retrieval (pH)	Species used for	Primary antibody concentration	Block	Secondary antibody	Secondary product #	Company	Secondary concentration	Method
Foxp2 Banham	-	-	-	mouse	9	All species	1:250	10% normal goat serum	Poly-HRP-GAM/R/R	VWRKDPVO55-HRP	Immunologic	1:2	Direct
RORB origene	TA806996	W001	Origene	mouse	9	All species	1:100	10% normal goat serum	Biotinylated Goat anti-mouse	BA-9200	Vector Labs	1:1000	ABC
CNTNAP2 Novus	NBP1-49575	1012	Novus biological	mouse	6	All species	1:200	10% normal goat serum	Biotinylated Goat anti-mouse	BA-9200	Vector Labs	1:1000	ABC
Foxp1 UMAB89	UM800020	W001	Origene	mouse	9	R. aegyptiacus	1:100	10% normal goat serum	Biotinylated Goat anti-mouse	BA-9200	Vector Labs	1:1000	ABC
Foxp1 ab134055	ab134055	GR97096-11	Abcam	rabbit	9	P. discolor	1:100	10% normal horse serum	Biotinylated Horse anti-rabbit	BA-1100	Vector Labs	1:1000	ABC
Foxp1 ab134055	ab134055	GR97096-11	Abcam	rabbit	9	Mouse	1:1000	10% normal horse serum	Biotinylated Horse anti-rabbit	BA-1100	Vector Labs	1:1000	ABC
TLE4 origene	TA330275	-	Origene	rabbit	9	All species	1:100	10% normal horse serum	Biotinylated Horse anti-rabbit	BA-1100	Vector Labs	1:1000	ABC

TABLE 2 Comprehensive description of gene expression patterns in *P. discolor*

		FoxP2		FoxP1		CntnaP2	
		Intensity	Abundance	Intensity	Abundance	Intensity	Abundance
Cerebral cortex	*Isocortex*						
	Cortex-layer I	-	-	-	-	-	-
	Cortex - layer II/III	+++	Rare	++++	Medium	+	Rare
	Cortex - layer IV	+++	Medium	++++	Abundant	+++	Rare
	Cortex-layerV	+++	Rare	++	Abundant	+++++	Abundant
	Cortex-layerVI	+	Rare	+++	Abundant	+	Medium
	Olfactory areas						
	Olfactory bulb, glomerular layer	+++++	Abundant	++	Rare	-	-
	Olfactory bulb, outer plexiform layer	++++	Rare	+	Rare	+++	Rare
	Olfactory bulb, mitral cell layer	++	Medium	+++	Medium	++++	Abundant
	Olfactory bulb, inner plexiform layer	+++	Rare	+++	Rare	+++	Rare
	Olfactory bulb, granule layer	++++	Rare	+	Rare	+++	Rare
	Anterior olfactory nucleus, external layer	+++	Rare	-	-	++++	Abundant
	Lateral olfactory tract	++++	Rare	-	-	-	-
	Nucleus of the lateral olfactory tract	-	-	-	-	++++	Medium
	Cortical sub-plate						
	Claustrum	-	-	-	-	+	Abundant
	Endopyriform nucleus	-	-	-	-	+	Abundant
	Posterior pyriform area	-	-	-	-	+++	Rare
	Lateral amygdaloid nucleus, pars anterior	-	-	++	Abundant	+	Medium
	Lateral amygdaloid nucleus, pars posterior	-	-	+++	Abundant	-	-
	Basolateral amygdaloid nucelus, anterior	+++	Abundant	+	Medium	+	Abundant
	Basolateral amygdaloid nucelus, posterior	-	-	+	Abundant	-	-
	Accessory basal amygdaloid complex	-	-	+	Rare	-	-
	Anterior amygdaloid area	+++++	Abundant	+++	Medium	+++	Rare
	Posterolateral cortical amygdaloid nucleus	-	-	-	-	+	Rare
	Hippocampal formation						
	CA1	++	Rare	+++	Abundant	+++	Abundant
	CA2	+	Rare	+++	Abundant	+++	Abundant
	CA3	+	Rare	+	Medium	+++	Abundant
	Dentate gyrus, polymorph layer	-	-	-	-	+++	Rare
	Dentate gyrus, ganule layer	-	-	-	-	-	-
	Subiculum	-	-	+++++	Abundant	+++	Rare

(Continues)

TABLE 2 (Continued)

		FoxP2		FoxP1		CntnaP2	
		Intensity	Abundance	Intensity	Abundance	Intensity	Abundance
Striatum	*Dorsal region*						
	Caudate nucleus	++++	Abundant	+++++	Abundant	++	Rare
	Putamen	++++	Abundant	+++++	Abundant	++++	Rare
	Ventral region						
	Nucleus accumbens	++++	Abundant	+++++	Abundant	+++	Rare
	Olfactory tubercle	++++	Abundant	+++++	Abundant	+++++	Medium
	Lateral septus						
	Lateral septal nucleus	++++	Abundant	+++	Medium	+	Rare
	Striatum-like Amygdala						
	Medial amygdaloid nucleus	++++	Abundant	-	-	++	Medium
	Central amygdaloid nucleus	+++	Rare	++	Abundant	-	-
	Intercalated amygdalar nucleus	+++++	Abundant	-	-	-	-
	Pallidum						
	Globus pallidus	++++	Rare	-	-	+++++	Medium
	Ventral pallidum	+++++	Abundant	-	-	-	-
	Substantia innominata	+++	Rare	-	-	+++	Abundant
	Medial septal nucleus	-	-	-	-	+++++	Abundant
	Diagonal band	-	-	+	Rare	+++++	Abundant
	Nuclear of the stria terminalis	++++	Rare	-	-	++	Rare
Thalamus	*Anterior group*						
	Anteroventral nucleus	-	-	-	-	++++	Abundant
	Anteromedial nucleus	-	-	-	-	++	Abundant
	Interanterodorsal nucleus	-	-	-	-	+++	Abundant
	Interanteromedial nucleus	+++	Medium	+	Medium	++	Abundant
	Laterodorsal nucleus	+	Rare	-	-	++++	Abundant
	Lateral group						
	Lateral posterior nucleus	+++	Abundant	-	-	+++	Abundant
	Posterior thalamic nucleus	+++	Abundant	+++	Medium	++	Abundant
	Suprageniculate nucleus	+++++	Abundant	-	-	+++	Abundant
	Medial group						
	Intermediodorsal nucleus	+++++	Abundant	+	Abundant	++	Abundant
	Mediodorsal thalamus	+	Abundant	-	-	+++	Abundant
	submedial nucleus of the thalamus	-	-	+++++	Medium	+++	Medium
	Midline group						
	Paraventricular nucleus	+++++	Abundant	+++	Abundant	+++	Abundant
	Paratenial nucleus	+++	Medium	-	-	+++	Abundant
	Nucleus reuniens*	+++	Medium	+++	Medium	+	Abundant
	Ventral nuclear group						
	Ventro anterial nucleus	-	-	+	Medium	+++	Abundant

(Continues)

TABLE 2 (Continued)

		FoxP2		FoxP1		CntnaP2	
		Intensity	Abundance	Intensity	Abundance	Intensity	Abundance
	Ventrolateral nucleus	+++	Abundant	+	Medium	+++	Abundant
	Ventromedial nucleus	+++	Rare	+++	Rare	++	Abundant
	Ventroposteromedial nucleus	+++	Abundant	-	-	++++	Abundant
	Ventroposterolateral nucleus	+++	Abundant	+++	Rare	++++	Abundant
	Intralaminar nuclei						
	Rhomboidal nucleus	+++++	Abundant	+++	Abundant	+	Abundant
	Centromedial nucleus	+++++	Abundant	+++	Medium	++	Abundant
	Paracentral nucleus	+++++	Abundant	-	-	++	Abundant
	Centrolateral nucleus	+++++	Abundant	-	-	+	Abundant
	Parafascicular nucleus	+++++	Abundant	+++++	Abundant	-	-
	Geniculate group						
	Lateral geniculate nucleus, dorsal	+++++	Medium	++	Rare	+++++	Abundant
	Lateral geniculate nucleus, ventral	+++++	Rare	+++	Medium	+++	Rare
	Medial geniculate nucleus, dorsal	+++	Abundant	-	-	+++	Abundant
	Medial geniculate nucleus, ventral	+++	Abundant	-	-	+++	Abundant
	Medial geniculate nucleus, magnocellular	+++++	Abundant	-	-	+++	Abundant
	Other						
	Reticular nucleus of the thalamus	-	-	-	-	++++	Abundant
	Subparafascicular nucleus	+++++	Abundant	+++++	Abundant	-	-
	Epithalamus						
	Habenular nucleus, medial	+++	Rare	-	-	++++	Medium
	Habenular nucleus, lateral	++	Rare	-	-	+++++	Medium
Hypothalamus	*Periventricular*						
	Paraventricular nucleus of hypothalamus	+++++	Abundant	++++	Medium	+++++	Abundant
	Supraoptic nucleus	++++	Medium	+++++	Abundant	++++	Abundant
	Arcuate	+++++	Medium	+	Medium	-	-
	Dorsomedial hypothalamic nucleus	++++	Abundant	-	-	++	Medium
	Median preoptic nucleus	+	Medium	++++	Rare	-	-
	Medial						
	Medial preoptic area	-	-	++++	Rare	+++	Abundant
	Anterior hypothalamic nucleus	+++++	Abundant	-	-	-	-
	Posterior hypothalamic nucleus	+++++	Medium	-	-	+	Medium
	Lateral						
	Lateral hypothalamic area	++	Medium	++	Medium	+	Medium
	Lateral preoptic area	+++++	Abundant	+++	Medium	+	Medium

TABLE 2 (Continued)

		FoxP2		FoxP1		CntnaP2	
		Intensity	Abundance	Intensity	Abundance	Intensity	Abundance
	Subthalamic nucleus	+++++	Abundant	+++	Rare	+++	Abundant
	Zona incerta, subthalamus	-	-	+++	Rare	++	Abundant
	Tuberal nucleus	++	Abundant	+	Abundant	-	-
Midbrain	**Sensory related**						
	Superior colliculus, superficial gray layer// optic layer	+++++	Medium	++	Rare	+++	Medium
	Inferior colliculus, external nucleus	++++	Rare	+++	Rare	+++	Rare
	Inferior colliculus	+++++	Abundant	+	Rare	++++	Abundant
	Parabigeminal nucleus	+++++	Abundant	-	-	-	-
	Motor related						
	Occulomotor nucleus	+++++	Rare	-	-	+++++	Abundant
	Midbrain reticular nucleus	+++++	Medium	++	Rare	++++	Abundant
	Superior colliculus, motor related	++++	Medium	++	Rare	++++	Abundant
	Ventral tegmental area	+++	Abundant	-	-	+++++	Abundant
	Periaqueductal gray	+++	Medium	+	Rare	++++	Medium
	Interstitial nucleus of Cajal	+++++	Medium	-	-	+++++	Medium
	Nucleus of Darkschewitsch	+++++	Abundant	-	-	+++++	Abundant
	Substantia nigra, reticular part	+++++	Medium	+++++	Medium	+++++	Abundant
	Anterior pretectal nucleus	++++	Abundant	++	Rare	++++	Abundant
	Nucleus of the posterior comissure	+++++	Medium	+	Rare	++++	Medium
	Olivary pretectal nucleus	++++	Medium	+	Medium	+++++	Medium
	Posterior pretectal nucleus	-	-	++	Rare	+++	Rare
	Red nucleus	-	-	-	-	+++	Abundant
	Behavioral state related						
	Substantia nigra, compact part	+++	Abundant	+	Rare	++++	Abundant
	Interfascicular nucleus Raphe	+++++	Abundant	+++	Medium	-	-
	Interpeduncular nucleus	-	-	-	-	+++	Medium
	Rostral linear Raphe nucleus	+++	Rare	-	-	-	-
	Central linear Raphe nucleus	++++	Rare	-	-	+++	Abundant
	Dorsal Raphe nucleus	+++++	Medium	+	Rare	+++++	Abundant
Hindbrain	**Pons sensory related**						
	Nucleus of the lateral lemniscus, dorsal and horizontal pa	+++++	Abundant	-	-	-	-
	Nucleus of the lateral lemniscus, ventral part	+++	Abundant	+++	Abundant	+++++	Abundant
	Periolivary complex	-	-	-	-	+++	Medium
	Pons motor related						
	Pontine reticular formation	++++	Rare	-	-	++++	Medium
	Pontine gray	-	-	-	-	+++++	Abundant
	Dorsal tegmental nucleus	+++	Medium	-	-	++++	Medium

(Continues)

TABLE 2 (Continued)

		FoxP2		FoxP1		CntnaP2	
		Intensity	Abundance	Intensity	Abundance	Intensity	Abundance
	Tegmental reticular nucleus	-	-	-	-	+++++	Abundant
	Pons behavioral state related						
	Superior central nucleus Raphe, medial part	+	Medium	+++	Rare	+++++	Abundant
	Superior central nucleus Raphe, lateral part	+++	Rare	-	-	++++	Medium
	Pontine reticular nucleus	+++++	Rare	+++	Rare	+++	Abundant
Cerebellum	*Cortex*						
	Molecular layer	-	-	-	-	-	-
	Purkinje cells	++++	Abundant	-	-	+	Medium
	Granular layer	-	-	-	-	+++++	Abundant

Egyptian fruit bats (*R. aegyptiacus*) originated from a breeding colony at UC Berkeley, Berkeley, CA. The specimens used in this study were imported from a breeding facility at the Weizmann institute in Israel or captured from a natural roost near Herzliya, Israel and imported to UC Berkeley. In this colony animals were kept under semi-natural conditions (12-hr day/12-hr night reverse daylight cycle, humidity 30–70% and temperature ranging between 70 and 75°F). Bats had free access to food and water. All experimental and breeding procedures were approved by the UC Berkeley Institutional care and use committee (IACUC).

2.2 | Sample collection

For both species, adult bats were housed in small groups in large cages and the juvenile *P. discolor* animal was caged separately with free access to food and water prior to sample collection. *P. discolor* were euthanized by an intraperitoneally (IP) applied lethal dose of pentobarbital (0.16 mg/g bodyweight). Brains were extracted and incubated in 4% formaldehyde solution (10% Formalin) for 48 hr. *R. aegyptiacus* were euthanized via an IP injection of 0.5 ml Beuthanasia-D solution (390 mg/ml sodium pentobarbital). Animals were then perfused with 200 ml of 0.025 M PBS + heparin (pH 7.4) followed by 200 ml of freshly prepared 4% paraformaldehyde in 0.025 M PBS (pH 7.4) delivered via a peristaltic pump. Subsequently, the brains were removed and stored in fixative (4% formaldehyde solution) for 48 hr. An adult male mouse was culled by cervical dislocation. The brain was extracted stored in fixative (4% formaldehyde solution) for $\sim$48 hr. Experimental procedures were approved by the Animal Ethics Committee of the Radboud University Nijmegen (Nijmegen, The Netherlands) and conducted in accordance with the Dutch legislation.

2.3 | Immunohistochemistry (IHC)

To generate a comprehensive view of the *P. discolor* and *R. aegyptiacus* brain, we generated serial sections of 4 μm thick tissue slices, with 49 and 45 slices per brain, respectively. Two adult males (> 1-year-old)

and one juvenile male ($\sim$2.5 months old) *P. discolor* animals, and one adult male (> 1-year-old) *R. aegyptiacus* animal were used to generate the images included in the online atlas. Further animals were used to confirm staining pattern. Nissl staining was used to show the structural features at each depth (see Figure 1 for *P. discolor* and Figure 2 for *R. aegyptiacus*). Adjacent slides were used in IHC (described below) to determine the expression pattern of FoxP2, FoxP1, and CntnaP2.

For IHC, brains were dissected into four parts (coronally), paraffin embedded and sliced into 4 μm thick sections and transferred to Superfrost plus glass slides (Menzel Gläser). The slides were dried overnight at room temperature and incubated at 57°C for 1 hr. For staining, the slides were washed in xylene for 10 min and re-hydrated sequentially in 100%, 95%, 70%, and 50% ethanol and water for 2 min/wash. Antigen retrieval was performed as indicated in Table 1—in either pH 6 citrate buffer (Immunologic) or pH 9 Tris-EDTA buffer (Immunologic) in a microwave for 3–5 min at 850W and 10 min at 180W. Endogenous peroxidase was blocked for 30min using 0.3% H_2O_2 (Sigma) diluted in water, followed by a brief wash in water. The tissue was then encircled with a PAP pen and blocked with 10% normal serum (Vector labs) for 1 hr at room temperature. After blocking, slides were incubated overnight at 4°C with primary antibody diluted in appropriate blocking solution (see Table 1). The following day, sections were washed three times with PBS and incubated with the corresponding secondary antibody for 1 hr at room temperature. All slides, except those used with the anti-Foxp2 antibody, were then processed for ABC-DAB staining. This involved incubation with avidin-biotin-horseradish peroxidase complex (ABC) using the Vectastain kit (Vector Laboratories). Briefly, reagent A and reagent B were diluted together 1:100 in PBS and incubated for 30 min at room temperature prior to addition to the tissue sections. Tissue sections were then incubated the ABC solution for 45 min at room temperature and washed three times in PBS. Experiments using anti-Foxp2 antibody did not need this step as the secondary antibody Poly-HRP-GAM/R/R (Immunologic) was already conjugated to horseradish peroxidase. Sections were then incubated for 7 min with diaminobenzidine (DAB) solution (Immunologic). Following color development the slides were briefly washed in water and counterstained with Haematoxylin

TABLE 3 Comprehensive description of gene expression patterns in *R. aegyptiacus*

		FoxP2		FoxP1		CntnaP2	
		Intensity	Abundance	Intensity	Abundance	Intensity	Abundance
Cerebral cortex	*Isocortex*						
	Cortex-layer I	-	-	-	-	-	-
	Cortex - layer II/III	-	-	++	Abundant	+	Abundant
	Cortex - layer IV	+	Abundant	++	Abundant	-	-
	Cortex - layer V	+++	Rare	++	Abundant	+++++	Abundant
	Cortex - layer VI	++++	Abundant	++	Abundant	+	Abundant
	Olfactory areas						
	Olfactory bulb, glomerular layer	+++++	Abundant	-	-	+	Rare
	Olfactory bulb, outer plexiform layer	+	Rare	-	-	+	Abundant
	Olfactory bulb, mitral cell layer	-	-	-	-	+++++	Abundant
	Olfactory bulb, inner plexiform layer	+++++	Rare	-	-	-	-
	Olfactory bulb, granule layer	+++++	Rare	-	-	+++	Rare
	Anterior olfactory nucleus	+++	Rare	++	Abundant	++	Abundant
	Anterior olfactory nucleus, medial	+++	Medium	++	Abundant	++	Abundant
	Anterior olfactory nucleus, dorsal	+++	Medium	++	Abundant	+	Abundant
	Anterior olfactory nucleus, lateral	-	-	++	Abundant	++++	Abundant
	Anterior olfactory nucleus, posteroventral	+++++	Rare	++	Abundant	++++	Abundant
	Anterior olfactory nucleus, external part	-	-	-	-	+++++	Abundant
	Nucleus of the lateral olfactory tract	-	-	-	-	+++	Abundant
	Cortical amygdalar area	+++	Medium	-	-	++++	Abundant
	Cortical sub-plate						
	Claustrum	-	-	-	-	+++	Medium
	Pyriform area, layer 2	-	-	-	-	+++++	Abundant
	Posterior pyriform area	-	-			-	-
	Lateral amygdaloid nucleus	-	-	+++++	Abundant	+++	Abundant
	Accessory basal amygdaloid complex	+++	Medium	-	-	+++	Abundant
	Anterior amygdaloid area	+++++	Medium	-	-	+++	Rare
	Hippocampal formation						
	CA1	+++	Abundant	+++++	Abundant	++++	Abundant
	CA2	-	-	+++	Abundant	++++	Abundant
	CA3	-	-	+	Abundant	++++	Abundant
	Dentate gyrus, polymorph layer	-	-	-	-	+++	Medium
	Dentate gyrus, ganule layer	-	-	-	-	+	Rare
	Subiculum	++++	Abundant	+++	Abundant	-	-

(Continues)

TABLE 3 (Continued)

		FoxP2 Intensity	FoxP2 Abundance	FoxP1 Intensity	FoxP1 Abundance	CntnaP2 Intensity	CntnaP2 Abundance
Striatum	*Dorsal region*						
	Caudate nucleus	++++	Abundant	+++++	Abundant	+	Rare
	Putamen	++++	Abundant	+++++	Abundant	+	Rare
	Ventral region						
	Nucleus accumbens	++++	Abundant	+++++	Abundant	+	Rare
	Olfactory tubercle	+++++	Abundant	++++	Abundant	+++	Medium
	Striatum-like Amygdala						
	Medial amygdaloid nucleus	++++	Abundant	+++	Rare	+++	Abundant
	Central amygdaloid nucleus	+++	Rare	+++	Medium	+++	Rare
	Intercalated amygdalar nucleus	+++++	Abundant	-	-	-	-
	Basal magnocellular nucleus	+++++	Abundant	-	-	-	-
	Pallidum						
	Globus pallidus	+++++	Rare	-	-	+++++	Medium
	Diagonal band	+++	Rare	-	-	+++++	Abundant
	Nuclear of the stria terminalis	++++	Medium	-	-	-	-
Thalamus	*Anterior group*						
	Anteroventral nucleus	-	-	-	-	+++	Abundant
	Anteromedial nucleus	-	-	-	-	+	Abundant
	Laterodorsal nucleus	-	-	-	-	-	-
	Lateral group						
	Lateral posterior nucleus	+++	Abundant	-	-	+	Abundant
	Posterior thalamic nucleus	+++	Abundant	+++	Abundant	+	Abundant
	Medial group						
	Mediodorsal thalamus	+++	Abundant	-	-	+	Rare
	Midline group						
	Paraventricular nucleus	+++++	Abundant	-	-	+	Abundant
	Nucleus reuniens*	+++++	Abundant	-	-	+++	Medium
	Ventral nuclear group						
	Ventro anterial nucleus	-	- Medium	-	-	+	Abundant
	Ventrolateral nucleus	+++	- Abundant	-	-	+	Abundant
	Ventromedial nucleus	-		++++	Abundant	-	-
	Ventroposteromedial nucleus	++++		++++	Abundant	+	Abundant
	Ventroposterolateral nucleus	-	-	++++	Abundant	+	Abundant
	Intralaminar nuclei						
	Rhomboidal nucleus	+++++	Abundant	++++	Abundant	+	Abundant
	Centromedial nucleus	+++++	Abundant	-	-	++	Abundant
	Paracentral nucleus	+++++	Abundant	-	-	++	Abundant
	Centrolateral nucleus	+++++	Abundant	-	-	+++	Abundant
	Parafascicular nucleus	+++++	Abundant	+++	Abundant	-	-

(Continues)

TABLE 3 (Continued)

		FoxP2		FoxP1		CntnaP2	
		Intensity	Abundance	Intensity	Abundance	Intensity	Abundance
	Geniculate group						
	Lateral geniculate nucleus, dorsal	++	Abundant	++	Rare	-	-
	Lateral geniculate nucleus, ventral	+++	Rare	++	Rare	+++	Abundant
	Medial geniculate nucleus, dorsal	++++	Abundant	-	-	-	-
	Medial geniculate nucleus, ventral	++++	Abundant	-	-	-	-
	Medial geniculate nucleus, magnocellular	+++	Abundant	-	-	-	-
	Other						
	Reticular nucleus of the thalamus	-	-	-	-	+++	Abundant
	Epithalamus						
	Habenular nucleus, medial	+++	Rare	-	-	+++++	Abundant
	Habenular nucleus, lateral	+++	Rare	-	-	+++++	Medium
Hypothalamus	*Periventricular*						
	Paraventricular nucleus of hypothalamus	+++	Medium	+++	Rare	+++++	Medium
	Supraoptic nucleus	++++	Abundant	+++++	Medium	+++++	Abundant
	Dorsomedial hypothalamic nucleus	-	-	-	-	-	-
	Lateral preoptic area	+++++	Medium	-	-	+	Medium
	Medial						
	Medial preoptic area	+++++	Medium	-	-	+++++	Abundant
	Ventromedial hypothalamic nucleus	+++	Rare	-	-	+++++	Abundant
	Medial eminence	+++++	Rare	-	-	+++++	Abundant
	Lateral						
	Lateral preoptic area	-	-	-	-	-	-
	Zona incerta, subthalamus	+++	Rare	-	-	-	-
Midbrain	*Sensory related*						
	Superior colliculus, superficial gray layer//optic layer	++++	Abundant	++	Rare	++	Medium
	Motor related						
	Superior colliculus, motor related	++++	Abundant	++	Rare	++	Medium
	Ventral tegmental area	+++++	Abundant	++	Rare	+++	Medium
	Periaqueductal gray	+++	Medium	++	Rare	++++	Medium
	Substantia nigra, reticular part	+++	Medium	+++	Medium	+++	Abundant
	Anterior pretectal nucleus	+++	Medium	-	-	++	Medium
	Behavioral state related						
	Substantia nigra, compact part	+++++	Abundant	-	-	+++	Abundant

(Continues)

TABLE 3 (Continued)

		FoxP2		FoxP1		CntnaP2	
		Intensity	Abundance	Intensity	Abundance	Intensity	Abundance
Cerebellum	*Cortex*						
	Molecular layer	-	-	-	-	-	-
	Purkinje cells	++++	Abundant	-	-	++	Medium
	Granular layer	-	-	-	-	+++++	Abundant

modified (Harris and Gill II) (Sigma) for 1 min. The slides where then washed in water, 50%, 70%, 95%, and twice in 100% ethanol, 2 min each wash. Finally, the slides where washed twice in Xylene (Sigma) and coverslipped using DPX (Sigma). An overview of all antibodies and conditions used can be found in Table 1.

2.4 | Antibody characterization

Primary antibodies were raised against human protein epitopes that were largely conserved with the relevant *P. discolor* and *R. aegyptiacus*

proteins. Details of the antibody conditions are given in Table 1 and full details of the antibodies and characterization are below. Secondary antibody-only controls were performed for all conditions and can be found in the online database (see https://hdl.handle.net/1839/84340C26-78EC-41BD-893B-12DE911BDA70@view).

FOXP2-Banham mouse monoclonal antibody, clone 73A/8, was raised against N-terminal epitope corresponding to amino acids 1–86 of the human protein, (this antibody was a generous gift of Alison Banham, but is also commercially available from Millipore Cat# MABE415; RRID: AB_2721039). The antiserum stains a single band of ~80 kDa
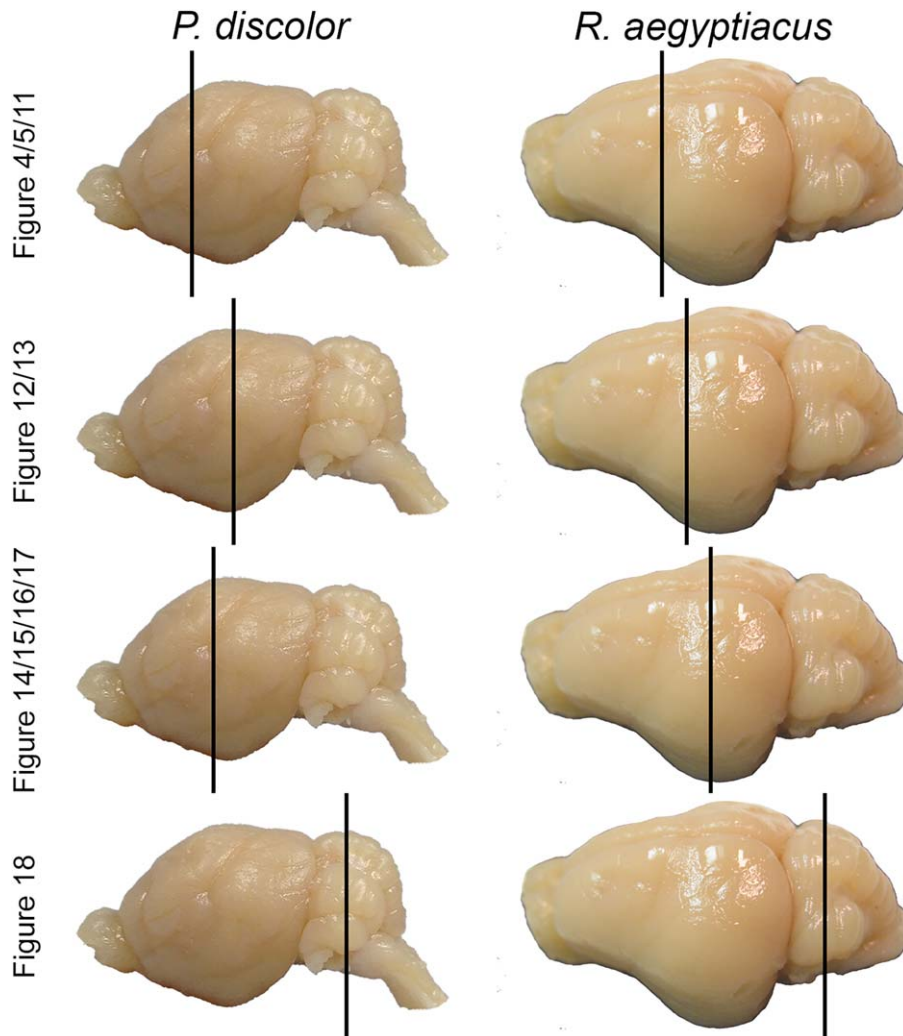

FIGURE 3 Whole dissected bat brains indicating depths of slices used for representative images. Side view of the *P. discolor* and *R. aegyptiacus* adult brains following whole brain dissection. The approximate brain depths used to display representative images in the main figures are indicated by the black lines
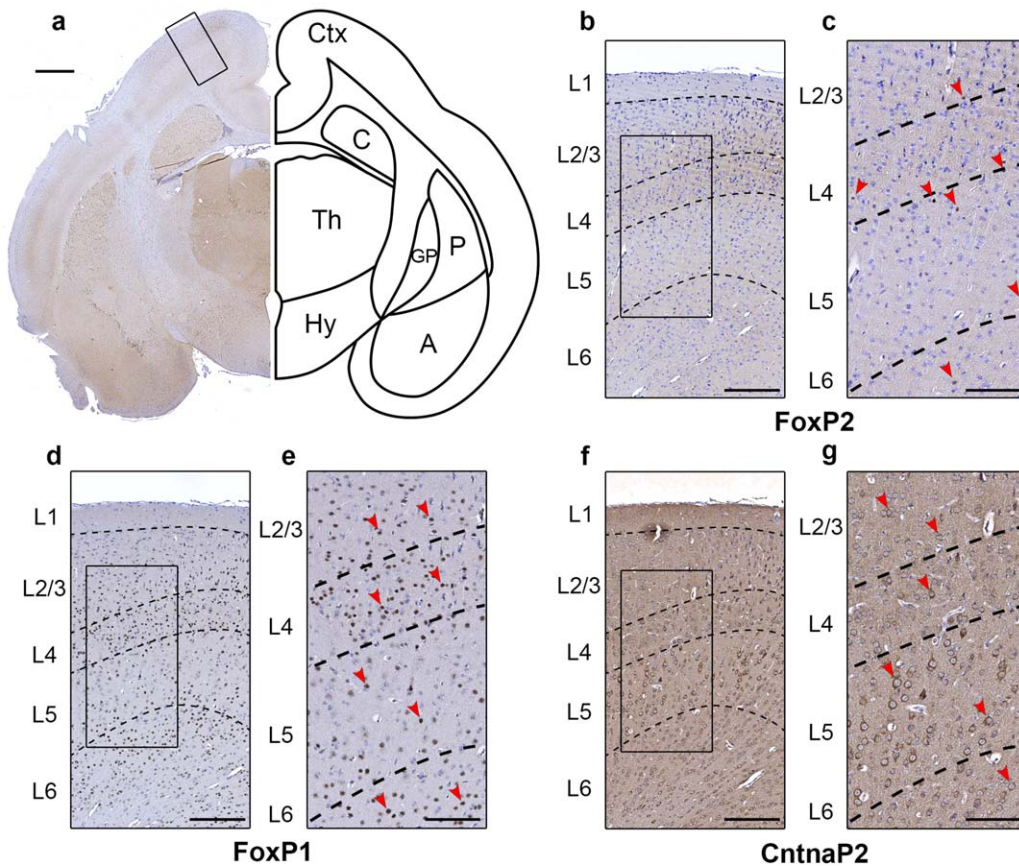
FIGURE 4 Examination of the *P. discolor* cortex reveals layer and species specific expression patterns. Structural overview of the *P. discolor* brain slice (immunostained against FoxP2) used to select inset boxes, including simplified line diagrams indicating key brain regions represented (a). See Figure 3 for an indication of slice depth. Inset boxes demonstrate representative immunostaining for FoxP2 (b, c), FoxP1 (d, e) and CntnaP2 (f, g). Note that FoxP2 and FoxP1 display nuclear localized staining, while Cntnap2 (Caspr2) displays a cytoplasmic/cell surface pattern of localization. High magnification panels for each gene (c, e, g) were included to facilitate visualization of details. Scale bar in panel (a) represents 1 mm, scale bars in (b, d, f) represent 250 μm and in (c, e, g) represent 125 μm. Red arrows indicate examples of positively stained cells. Brain structures are abbreviated as follows; Cortex (Ctx), Caudate (C), Putamen (P), Globus Pallidus (GP), Thalamus (Th), and Hypothalamus (Hy)

on Western blot (manufacturers' technical information). Staining with this antibody gave broadly the same staining pattern of immunoreactivity and mRNA expression pattern that has been described previously (Ferland et al., 2003; Lai et al., 2003), apart from the exceptions noted in the results below (e.g., reduced cortical staining in *P. discolor*). No staining was seen when the antibody was used to stain brain tissue from a Foxp2 knockout mouse (see https://hdl.handle.net/1839/8C1733D7-DA9A-4776-AEC6-0612CB7B0655@view).

Two antibodies were used for FoxP1 detection. The FOXP1 mouse monoclonal antibody, clone UMAB89 (Origene Cat# UM800020, RRID: AB_2629133), was raised against the full length recombinant human FOXP1 protein (NP_116071). The antiserum stains a single band of ∼75 kDa molecular weight on Western blot (manufacturers' technical information). The FOXP1 rabbit monoclonal clone EPR4113 (AbCam Cat # AB134055, RRID: AB_2632402) was raised against an epitope available upon request from the company. The antiserum stains a single band of ∼75 kDa molecular weight on a Western blot (see https://hdl.handle.net/1839/70A28CEC-9FA6-4058-B810-33B411090220@view). Staining with both these FOXP1 antibodies gave the same staining pattern of

immunoreactivity and mRNA expression pattern that has been described previously (Ferland et al., 2003).

CNTNAP2 (CASPR2) mouse monoclonal antibody, clone S67-25 (Novus Biological Cat #NBP1–49575, RRID: AB_10011672), was raised against a fusion protein corresponding to amino acids 96–1265 of human CASPR2. The antiserum stains a single band of ∼180 kDa molecular weight on Western blot (manufacturers' technical information). Staining with this antibody gave the same staining pattern of immunoreactivity and mRNA expression pattern that has been described previously (Bakkaloglu et al., 2008; Gordon et al., 2016).

TLE4 rabbit polyclonal antibody (Origene Cat #TA330275, RRID: AB_2721043) was raised against synthetic peptide directed toward the N-terminal of human protein corresponding to amino acids 215–264. The antiserum stains a single band of ∼84 kDa and a second band at ∼30 kDa molecular weight on Western blot (manufacturers' technical information). TLE4 was used as a layer marker for cortical layer 6 and staining with this antibody gave the same layer 6 specific staining pattern of immunoreactivity that has been described previously (Hevner, 2007; Nakagawa et al., 2017).
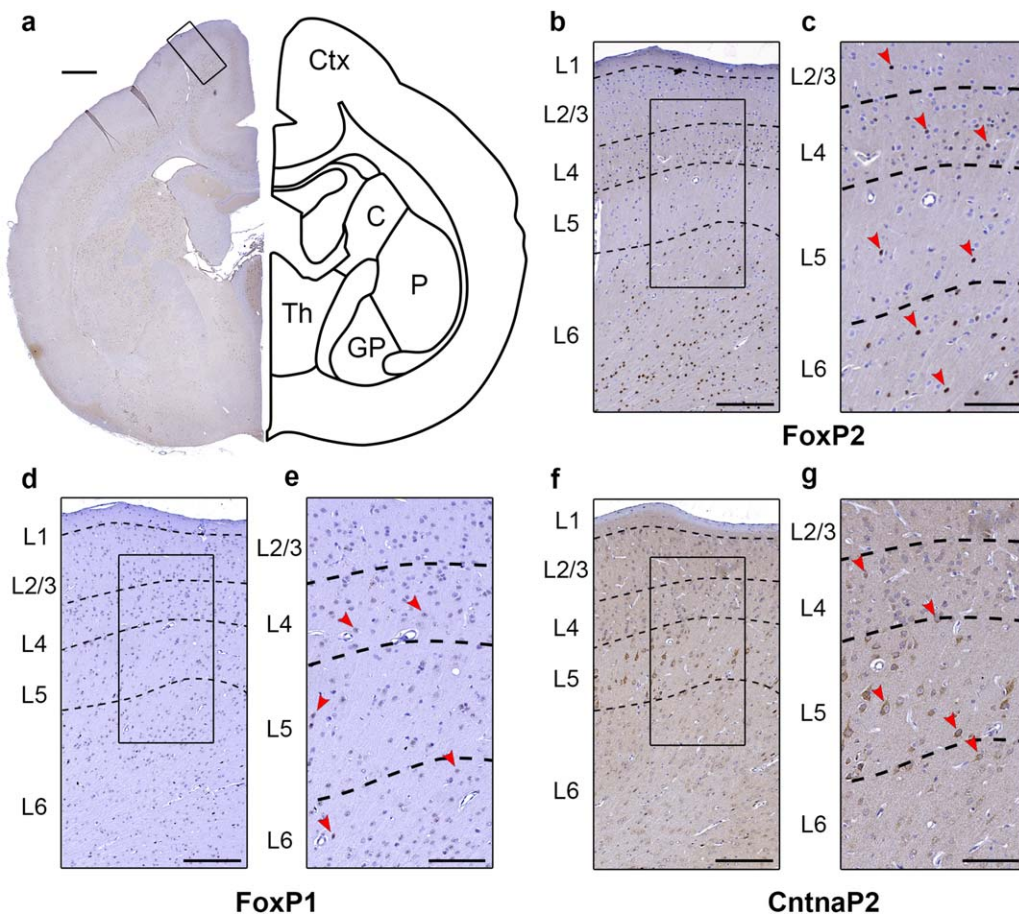
FIGURE 5 Examination of the *R. aegyptiacus* cortex reveals layer and species specific expression patterns. Structural overview of the *R. aegyptiacus* brain slices (immunostained against FoxP2) used to select inset boxes, including simplified line diagrams indicating key brain regions represented (a). See Figure 3 for an indication of slice depth. Inset boxes demonstrate representative immunostaining for FoxP2 (b, c), FoxP1 (d, e) and CntnaP2 (f, g). High magnification panels for each gene (c, e, g) were included to facilitate visualization of details. Scale bar in panel (a) represents 1 mm, scale bars in (b, d, f) represent 250 μm and in (c, e, g) represent 125 μm. Red arrows indicate examples of positively stained cells. Brain structures are abbreviated as follows; Cortex (Ctx), Caudate (C), Putamen (P), Globus Pallidus (GP), Thalamus (Th), and Hypothalamus (Hy)

RORB mouse monoclonal antibody, clone OTI1G1 (Origene Cat#TA806996, RRID: AB_2721044), was raised against a human recombinant RORB protein fragment corresponding to amino acids 1–260. The antiserum stains a single band of ∼52 kDa molecular weight on Western blot (manufacturers' technical information). RORB was used as a layer marker for cortical layer 4 and staining with this antibody gave the same layer 4 specific staining pattern of immunoreactivity that has been described previously (Hevner, 2007; Moroni et al., 2009; Jabaudon, Shnider, Tischfield, Galazo, & Macklis, 2012).

2.5 | Expression analysis and region identification

To make a comprehensive record of expression, 12 representative sections at different tissue depths across the brain were analyzed in detail (indicated by asterisks in Figures 1 and 2). For each brain region, the expression was graded for staining intensity (absent to high: - to +++++) and abundance of positive cells in a region ("Rare" to

"Abundant"). Scoring was made across the cerebral cortex, striatum, thalamus, hypothalamus, midbrain, hindbrain, and cerebellum. To aid in analysis of the *R. aegyptiacus* brain structures, two anatomical brain atlases were mainly used, Schneider R: Das Gehirn von *R. aegyptiacus* (Schneider, 1966) and an unpublished atlas shared by Yartsev, M. (personal communication, prepared in the laboratory of Nachum Ulanovsky at the Weizmann institute, Israel). There are no published atlases for *P. discolor*, so for this species we used the brain atlas of the closely related species *Carollia perspicilatta* for analysis (Scalia, 2013). For identification of different subfields of the auditory cortex of *P. discolor* we used data published in Hoffmann, Firzlaff, Radtke-Schuller, Schwellnus, and Schuller (2008). Where these atlases were incomplete or ambiguous, additional resources were used including the Allen mouse brain atlas (Lein et al., 2007), and the *Rosettus amplexicaudatus brachyotis* (Baron, Stephan, & Frahm, 1996) brain atlas. Complete analysis of staining can be found in Table 2 (*P. discolor*) and Table 3 (*R. aegyptiacus*). Depths of images represented in manuscript figures are indicated in Figure 3.
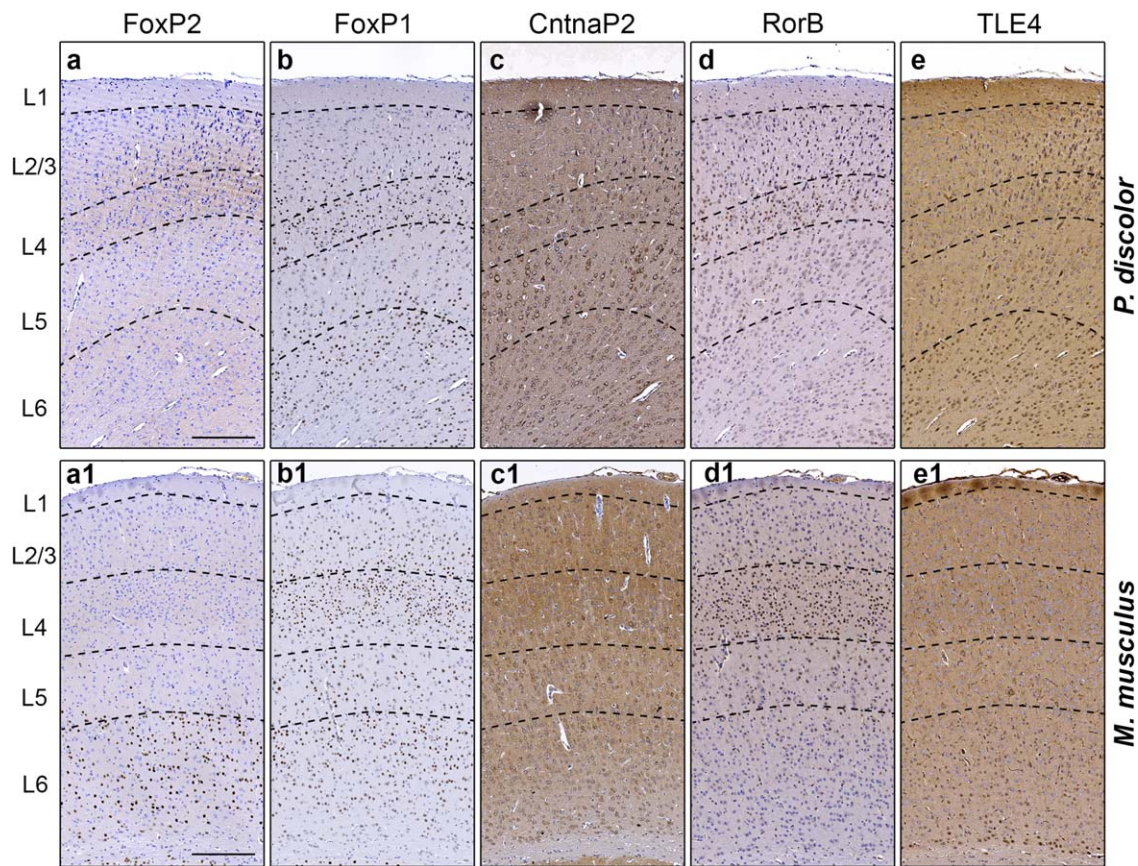
FIGURE 6 Cortical layering is conserved between mouse brains and *P. discolor* bats. *P. discolor* (a–e) and *M. musculus* (a1–e1) brains were stained for FoxP2 (a-a1), FoxP1 (b-b1) and CntnaP2 (c-c1). The pattern of standard cortical markers was also compared across species including RORB—a layer 4 cortical marker (d-d1) and TLE4—a layer 6 cortical marker (e-e1). Dotted lines represent boundaries between the cortical layers that were determined based on RORB and TLE4 expression, as well as cellular morphology. All genes and layer markers showed consistent distribution in the cortex across mouse and *P. discolor*, except for FoxP2. Scale bar represents 250 μm

2.6 | Image preparation and tagging

Slides were scanned using either a Sakura VisionTek Live Digital Microscope scanner or Axio2 Zeiss miscroscope to a resolution of 0.55 μm/pixel and 0.45 μm/pixel, respectively. Images were globally white balanced equally among all sections that were stained with the same antibody to match the histological slides using Photoshop CS6. Images were then meta-tagged for; species, age, experimental conditions (primary antibody, antibody concentration, antigen retrieval pH, IHC method), slicing plane, and the main brain regions, for example, cortex, striatum, and thalamus.

3 | RESULTS

We found expression of FoxP2, FoxP1, and CntnaP2 in the brains of both bat species throughout multiple regions. Expression patterns were highly conserved across the two vocal learning bat species, with a few key exceptions, which are discussed region by region, below. A summary of the expression patterns found in *P. discolor* can be found in Table 2, and *R. aegyptiacus* in Table 3.

3.1 | Cerebral cortex

FoxP2, FoxP1, and CntnaP2 were all expressed in the cerebral cortex of both species, with differing layer specific expression patterns (Figures 4, 5). FoxP1 and CntnaP2 did not show species-specific differences in distribution across the six layers of the cortex, however FoxP2 displayed dramatic differences between *P. discolor* and *R. aegyptiacus*.

Rousettus aegyptiacus displayed strong and abundant expression of FoxP2 in layer 6 and deep layer 5 neurons (Figure 5a–c), consistent with the pattern found in the adult rodent cortex (see Figure 6). Strong and abundant staining was also found in layer 4 neurons in some regions of the *R. aegyptiacus* cortex along with sparse but intense staining of occasional neurons in layers 2–3. Strikingly, in adult *P. discolor* bats, FoxP2 expression was not enriched in layer 6. Instead, FoxP2 could only be identified in rare neurons spread across layers 2–6 of the cortex (Figure 4a–c). In both species, the FoxP2 protein was strongly detected in other brain regions in comparable patterns, and protein detection was confirmed via western blot (see https://hdl.handle.net/1839/BF738ABE-E1C2-4B90-9752-47A1EF671B21@view), showing that this difference was unlikely to be due to antibody/epitope recognition differences across the species. Given these differences, we
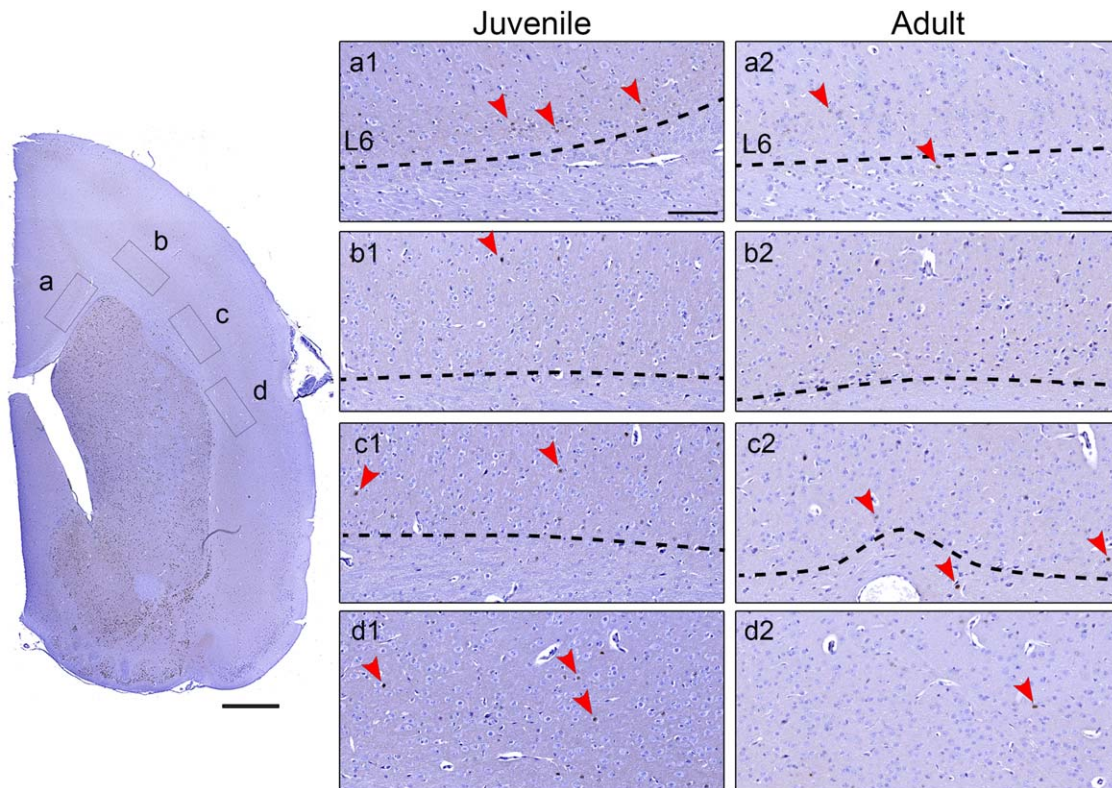
FIGURE 7 Distribution of FoxP2 in layer 6 of the juvenile vs. adult *P. discolor* cortex. Anterior brain slice (rostral-caudal distance ~3,700 μm) was chosen to illustrate representative FoxP2 protein expression in this cortical region which roughly corresponds to the location of the somatosensory cortex in other bat species. Comparable depths were used for both juvenile (~2.5 months old) and adult (>1 year old) brains. Inset boxes (a–d) indicate the location of the high magnification images for juvenile (a1–d1) and adult (a2–d2) brains. Only rare and weak staining can be observed in these regions of the cortex in both juvenile and adult animals. Scale bar in left panel (a–d) represents 1 mm, and scale bars in panels (a1–a2) represent 125 μm. Broken lines indicate the boundary between layer 6 (L6) and the corpus callosum. Red arrows show examples of positively stained cells

compared layer specific markers between mouse and *P. discolor* brains. These classical markers of layer 4 and 6 (RORB and TLE4, respectively) indicated conservation of the broad cortical layering between mouse and *P. discolor* (Figure 6) suggesting that the FoxP2 expression differences observed in *P. discolor* did not reflect major differences in the development of cortical layering. As both *P. discolor* brains tested were male, we also compared staining in two female brains and observed the same pattern of cortical expression (data not shown).

To determine if the expression pattern observed in *P. discolor* was consistent throughout development or a feature of adult animals, we compared expression of FoxP2 in juvenile (~2.5 months old) and adult brains. In juvenile *P. discolor*, enrichment of FoxP2 in layer 6 could be observed, but this varied across cortical areas (rostro-caudal and dorso-ventral). To illustrate this variation across the cortex, we compared expression in juvenile and adult at four different rostro-caudal depths, and four different dorsal–ventral positions per depth (Figures 7–10). FoxP2 positive neurons were abundant at a number of positions in the juvenile cortex (e.g., Figures 8a1–b1, 9a1–b1, 10b1–d1), but only sparse FoxP2 positive layer 6 neurons were observed in the adult (Figures 7–10, panels a2-d2). Some of the highest enrichment of layer 6 FoxP2 expression in the juvenile auditory cortex was found in regions that roughly correspond to the posterior dorsal field (PDF, Figure 10b1) and the primary auditory cortex (Figure 10c1–d1) (Hoffmann

et al., 2008). By comparison, staining was not visible in the primary auditory cortex of adult *P. discolor* (Figure 10b2–c2).

In both species, FoxP1 was observed across layers 2–6 (Figures 4, 5, panels d, e), consistent with the rodent expression pattern (Figure 6b1). The staining appears weaker in the *R. aegyptiacus* cortex in Figure 5d, e, although high resolution images (see online database for *R. aegyptiacus*) clearly show that expression is present in a large number of neurons throughout the layers with a distribution comparable to *P. discolor* and mouse (see Figure S4d-e and Figure 6b-b1). Differences in intensity may be due to the different FoxP1 antibody used for *R. aegyptiacus* (see Table 1) since when this antibody was tested on *P. discolor* or mouse tissue, weaker staining was also observed in some parts of the cortex compared to other brain regions (data not shown). CntnaP2 was also expressed across layers 2–6 of the cortex of both species, with the strongest and most abundant expression found in layer 5 and sparse expression observed in other layers (Figures 4–5, panels f, g). This was consistent with the expression pattern of Cntnap2 observed in the mouse cortex (Figure 6c-c1).

3.2 | Striatum

FoxP1 and FoxP2 showed strong and highly overlapping patterns of expression throughout the striatum, both being found abundantly in
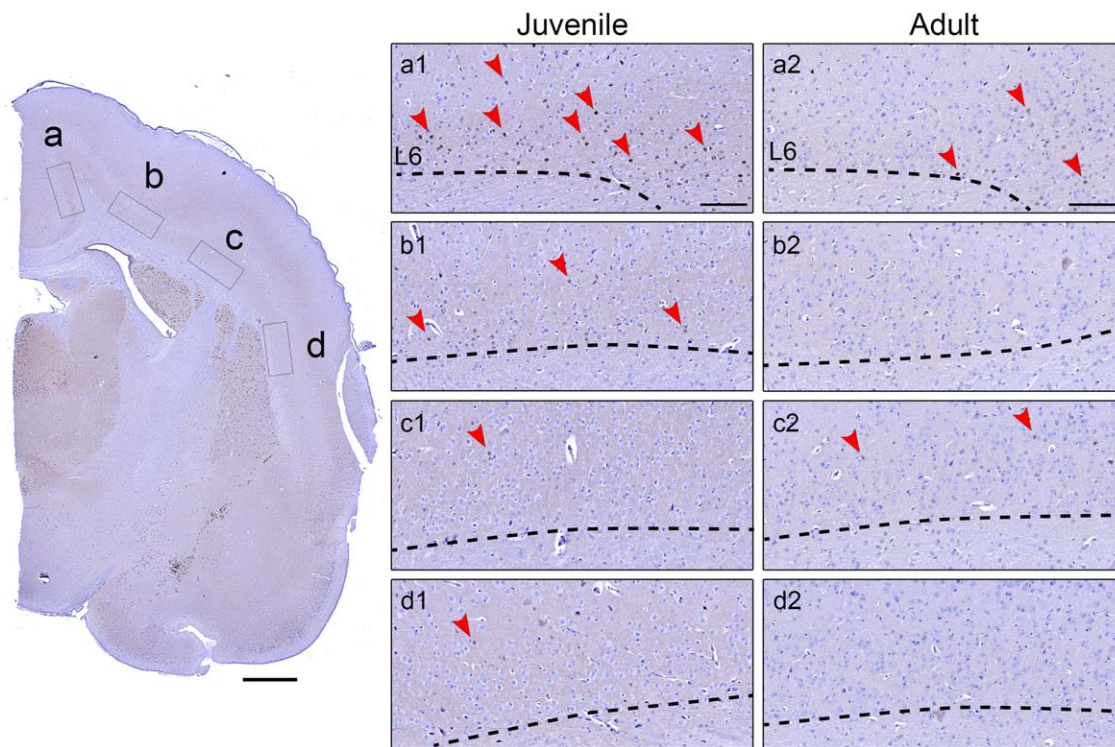
FIGURE 8 Distribution of FoxP2 in layer 6 of the juvenile vs. adult *P. discolor* cortex. Anterior brain slice (rostral–caudal distance ∼5,900 µm) was chosen to illustrate representative FoxP2 protein expression in this cortical region. Comparable depths were used for both juvenile (∼2.5 months old) and adult (>1 year old) brains. Inset boxes (a–d) indicate the location of the high magnification images for juvenile (a1–d1) and adult (a2–d2) brains. The juvenile *P. discolor* cortex shows abundant layer 6 FoxP2 expression in section a1 and moderate expression in b1, compared to the rare layer 6 expression observed in the comparable adult sections (a2, b2). Only rare expression was observed in juvenile (c1–d1) or adult (c2–d2) in other regions of the cortex, which roughly correspond to the anterior dorsal and anterior ventral fields (ADF, AVF) of the auditory cortex in *P. discolor*. The ADF is non-tonotopically organized and contains neurons mainly tuned to frequencies of the echolocation calls of *P. discolor* (40–90 kHz). The AVF is tonotopically organized with the frequency gradient running opposite to the gradient in primary auditory cortex (i.e., low frequencies are located at the rostral border). The AVF might represent the anterior auditory field described in other mammals (Hoffmann et al., 2008). Regions (a) and (b) might be considered as secondary auditory areas adjacent to the ADF in *P. discolor* but have not been characterized anatomically or functionally, so far. Scale bar in left panel (a–d) represents 1 mm, and scale bars in panels (a1–a2) represent 125 µm. Broken lines indicate the boundary between layer 6 (L6) and the corpus callosum. Red arrows show examples of positively stained cells

the caudate nucleus, putamen, nucleus accumbens, olfactory tubercle, and lateral septal nucleus in both species (Figure 11). FoxP1 expression was never seen in the globus pallidus (Figure 11c, d), however intense staining of FoxP2 could be found, but only in very rare cells (Figure 11a, b). By comparison, CntnaP2 showed a largely inverse regional pattern of expression with only rare staining in the caudate nucleus and putamen, but abundant and intense staining in the globus pallidus and other regions of the pallidum (Figure 11e, f). Both weakly and intensely stained striatal neurons were observed for FoxP2 and FoxP1, which is of interest for future follow up since weak versus intense FoxP2 levels have been related to age and singing behavior in songbirds (Thompson et al., 2013).

3.3 | Hippocampus

The hippocampus was another region for which differences in FoxP2 expression were observed between the species. In *P. discolor*, FoxP2 was not expressed in the hippocampus, except for some very rare, mostly weak staining in CA1–3 (Figure 12a–f). However in *R.*

aegyptiacus, FoxP2 was strongly and abundantly expressed in CA1 and the subiculum, but not found at all in other hippocampal regions (Figure 13a–f). Expression of FoxP1 and CntnaP2 was largely conserved across *P. discolor* and *R. aegyptiacus*. In both species, FoxP1 was abundantly found throughout neurons of CA1, CA2, CA3, and the subiculum (Figures 12, 13, panels g–j). Staining in CA3 was weaker (Figures 12, 13, panel i) compared to the very strong staining observed in the other regions. In both species CntnaP2 staining was strong and abundant throughout the hippocampus (Figures 12, 13, panels k–n). A small difference was observed between the species in that CntnaP2 could be found in some rare cells of the subiculum in *P. discolor*, but not in *R. aegyptiacus*.

3.4 | Thalamus

Staining in the Thalamus was largely conserved across both species (Figures 14, 15), with a few exceptions in the ventral nuclear (differences in all three genes) and geniculate (differences in CntnaP2) groups of nuclei. FoxP2 expression was widespread and intense in the
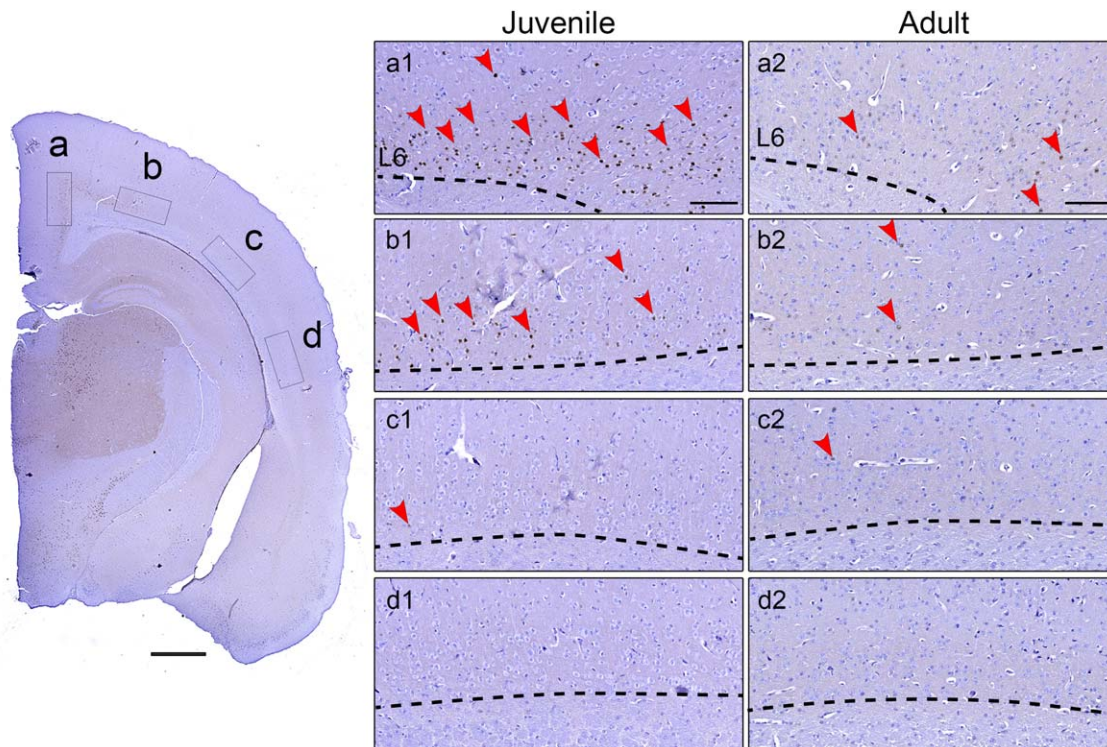
FIGURE 9 Distribution of FoxP2 in layer 6 of the juvenile versus adult *P. discolor* cortex. Posterior brain slice (rostral–caudal distance ∼8,000 μm) was chosen to illustrate representative FoxP2 protein expression in this cortical region. Comparable depths were used for both juvenile (∼2.5 months old) and adult (>1 year old) brains. Inset boxes (a–d) indicate the location of the high magnification images for juvenile (a1–d1) and adult (a2–d2) brains. The juvenile *P. discolor* cortex shows strong and abundant layer 6 FoxP2 expression in section a1 and b1, compared to the rare layer 6 expression observed in the corresponding adult sections (a2, b2). Only rare expression was observed in juvenile (c1–d1) or adult (c2–d2) in other regions of the cortex at this depth. Regions (a) and (b) might be considered as secondary auditory areas adjacent to the posterior dorsal auditory field (PDF) in *P. discolor* but have not been characterized anatomically or functionally, so far. Scale bar in left panel (a–d) represents 1 mm, and scale bars in panels (a1–a2) represent 125 μm. Broken lines indicate the boundary between layer 6 (L6) and the corpus callosum. Red arrows show examples of positively stained cells

thalamus, being most abundant in the lateral, midline, ventral, intralaminar, and geniculate nuclei (Figures 14, 15, panels a, b, c1, d1, e1). A small species difference could be observed in the ventroposterolateral nucleus of the ventral nuclear group where abundant, moderate intensity expression was observed in *P. discolor*, but no expression was found in *R. aegyptiacus*. FoxP1 was also found throughout the thalamus often overlapping with FoxP2 expression. Although FoxP1 was generally less abundant and less intense in its staining pattern than FoxP2 (Figures 14, 15, panels c2, d2, e2), it is possible that this is due to antibody/epitope differences. Cntnap2 was abundantly expressed in both species throughout the nuclei of the thalamus (Figures 14, 15, panels c3, d3, e3). One clear CntnaP2 expression difference between the species was found in the geniculate group of nuclei, where CntnaP2 was abundant in almost all nuclei in *P. discolor*, but absent in all but the ventral lateral geniculate nucleus in *R. aegyptiacus*.

3.5 | Amygdala

In the amygdala, FoxP1 and FoxP2 tended to show inverse patterns of expression (Figures 16c–j, c1-j1 and 17c–h, c1-h1). In both species, FoxP2 expression was low in the anterior lateral amygdaloid nucleus

(La; Figures 16c and 17c), where FoxP1 expression was high (Figures 16c1 and 17c1). Conversely FoxP2 expression was high but FoxP1 expression was low in the anterior basolateral (BLa; Figure 16e-e1) or basal amygdaloid nuclei (Bmg; Figure 17d-d1), medial amygdaloid nucleus (Me) (Figures 16h-h1 and 17g-g1), and intercalated amygdaloid nucleus (IA) (Figures 16i-i1 and 17e-e1). FoxP1 and FoxP2 were both expressed in the central amygdaloid nucleus (Ce) (Figures 16g-g1 and 17f-f1). CntnaP2 was not strongly expressed in the amygdala (Figures 16c2-j2 and 17c2-h2), except for in a few regions in *R.aegyptiacus* including the La (Figure 17c2), Me (Figure 17g2) and accessory basal amygdaloid nucleus (AB) (Figure 17h2). In contrast CntnaP2 staining was weak and sparse in these regions in *P. discolor*.

3.6 | Cerebellum

In both species, FoxP2 was restricted to the Purkinje cell layer of the cerebellum (Figure 18c, d), whereas FoxP1 was not expressed at all in the cerebellum (Figure 18e, f). Cntnap2 was observed in Purkinje cells and in the granular layer, but not in cells of the molecular layer (Figure 18g, h). No species-specific differences were observed in the cerebellum for any of the genes tested.
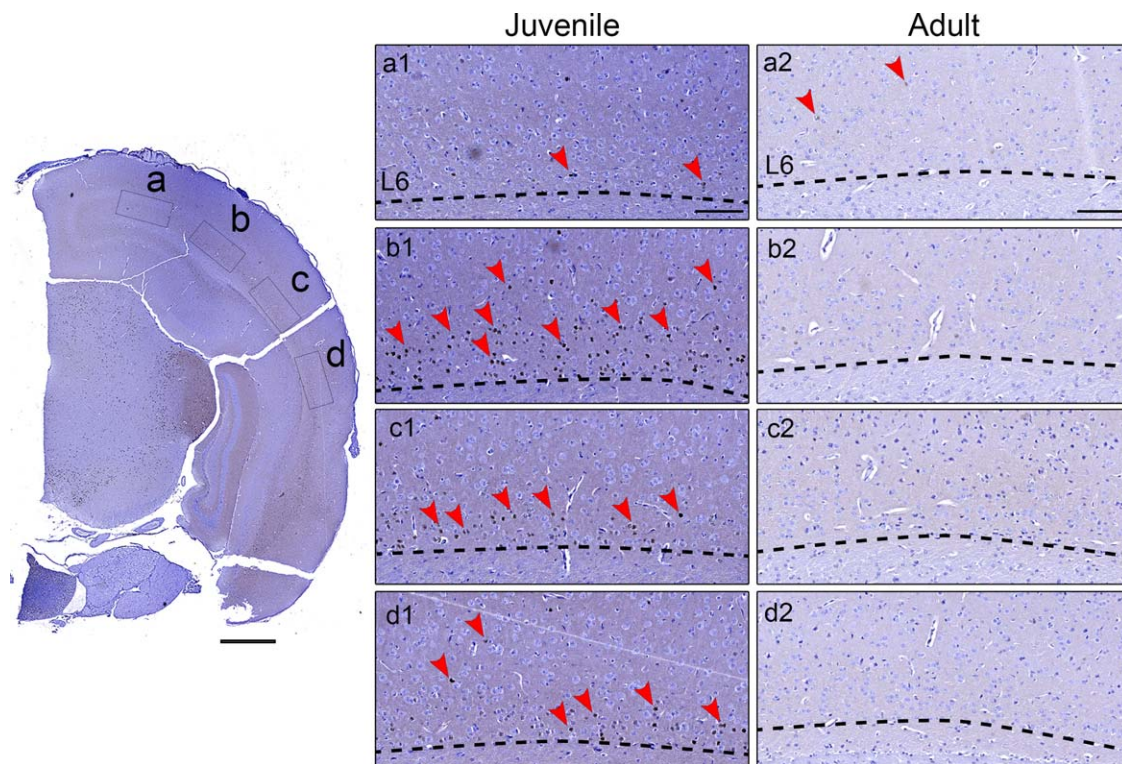
FIGURE 10 Distribution of FoxP2 in layer 6 of the juvenile versus adult *P. discolor* cortex. Posterior brain slice (rostral-caudal distance ∼8,900 μm) was chosen to illustrate representative FoxP2 protein expression in this cortical region. Comparable depths were used for both juvenile (∼2.5 months old) and adult (>1 year old) brains. Inset boxes (a–d) indicate the location of the high magnification images for juvenile (a1–d1) and adult (a2–d2) brains. Juvenile (a1) and adult (a2) *P. discolor* regions show little FoxP2 expression in region (a) of the cortex at this depth. The juvenile *P. discolor* cortex shows strong and abundant layer 6 FoxP2 expression in sections b1 and c1 and moderate expression in d1. No Foxp2 positive cells could be found in corresponding adult brain regions (b2–d2). Region (b) roughly corresponds to the posterior dorsal field (PDF) of the auditory cortex and regions (c, d) roughly correspond to the primary auditory cortex of *P. discolor*. Scale bar in left panel (a–d) represents 1 mm, and scale bars in panels (a1–a2) represent 125 μm. Broken lines indicate the boundary between layer 6 (L6) and the corpus callosum. Red arrows show examples of positively stained cells

3.7 | Open access database of expression via the online "Batlas" portal

All high resolution images are viewable via a persistent online open access database. This database contains the Nissl stained sections and the IHC staining for FoxP1, FoxP2, and CntnaP2 in two adult and one juvenile *P. discolor* and one adult *R. aegyptiacus* brain. The interactive database allows images to be browsed by species (*P. discolor* or *R. aegyptiacus*), age (adult or juvenile) or staining (FoxP1, FoxP2 CntnaP2, or Nissl staining) and have been meta-tagged to facilitate image searches based on these properties, on experimental conditions, or on the key brain regions represented in each image. These high resolution images allow viewing at high magnification (0.45–0.55 μm/pixel), making it possible to view expression at the level of individual neurons and observe the often subtle detail of expression patterns across brain regions. The BATLAS database can be accessed by the persistent link: https://hdl.handle.net/1839/00-5B1D28A0-32AF-4DD4-8868-4404 EC75EDAA@view which will take browsers to the root of the database. To view images it is then necessary to either search the database for relevant tags (e.g., FoxP2, adult), or expand the file tree (via + symbol) to the relevant image or group of images (e.g., Batlas→

Bat Immuno→ *Phyllostomus discolor*→ Adult #1→ FoxP2→ Coronal→ *P.discolor* FoxP2-Banham).

4 | DISCUSSION

To learn new vocalizations animals must identify and recognize relevant sounds, hold these sounds in memory as a vocal template, enact a motor program to mimic these sounds, use feedback to determine "goodness of fit", and modify the motor output as appropriate to accurately match the template. As such, VPL must, by necessity, involve multiple brain regions and neural circuits underlying sensorimotor perception, integration, memory, and motor production (amongst others) (Brainard & Doupe, 2000; Mooney, 2009; Bolhuis et al., 2010). Although the neural circuits involved in bat vocal learning are not yet defined, work investigating these individual components and studies of vocal learning in songbirds, have highlighted regions of interest for mammalian vocal learning (Jarvis, 2007; Bolhuis et al., 2010; Petkov & Jarvis, 2012). Herein, we report detailed expression patterns of three key language-related genes in the brains of vocal learning bats. All three genes (FoxP2, FoxP1, and CntnaP2) were expressed across many brain regions, but in specialized patterns within neuronal subtypes.
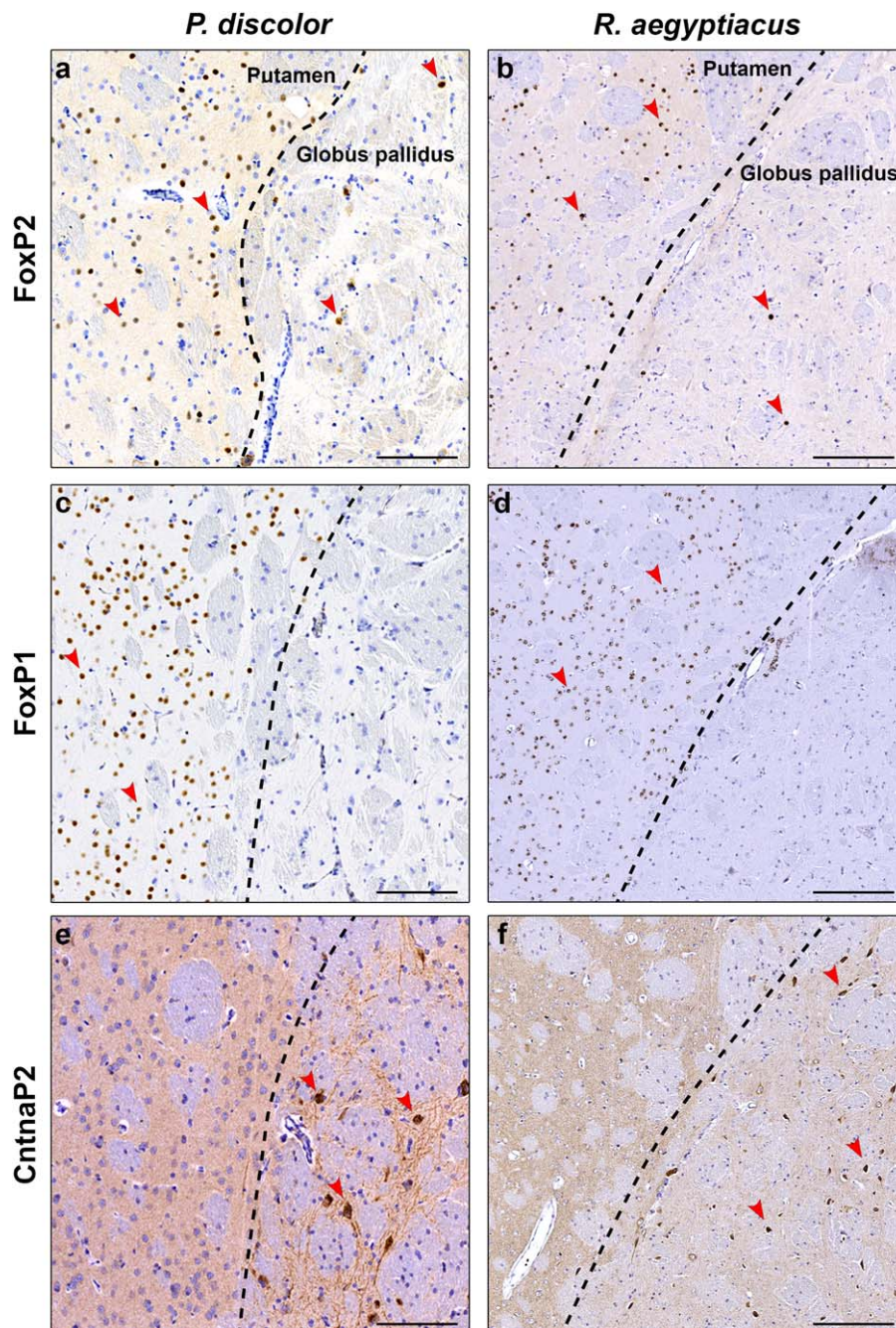
FIGURE 11 FoxP genes show an inverse expression pattern to CntnaP2 in compartments of the striatum of both bat species. High magnification images were taken from the brain slices at the depth indicated in Figure 3, which is the same depth as for Figure 4 (*P. discolor*) and 5 (*R. aegyptiacus*). Representative IHC images for FoxP2 (a, b) and FoxP1 (c, d) demonstrate strong expression in the putamen, but not in the globus pallidus. Conversely CntnaP2 is strongly expressed in the globus pallidus but not in the putamen (e, f). Broken lines illustrate the boundary between putamen and globus pallidus and red arrows indicate examples of positively stained cells. Scale bars represent 125 μm for *P. discolor* panels (a, c, e) and 250 μm for *R. aegyptiacus* panels (b, d, f)

4.1 | Forebrain circuits relevant for vocal learning—auditory circuitry

The auditory cortex is the region of the cortex primarily responsive to sound and the primary (AI) and anterior auditory (AAF) fields tend to have tonotopic organizations in mammals (Ehret, 1997; Rauschecker, 1998), including bats (Dear, Fritz, Haresign, Ferragamo, & Simmons, 1993; Esser & Eiermann, 1999; Hoffmann et al., 2008; Ulanovsky & Moss, 2008). Audio-vocal control in bats and other mammals involves connections between the auditory cortex, anterior cingulate cortex (ACC), primary orofacial motor cortex, and supplementary motor areas of the cortex as well as subcortical and midbrain regions (Jurgens, 2002, 2009; Loh, Petrides, Hopkins, Procyk, & Amiez, 2016; Roberts
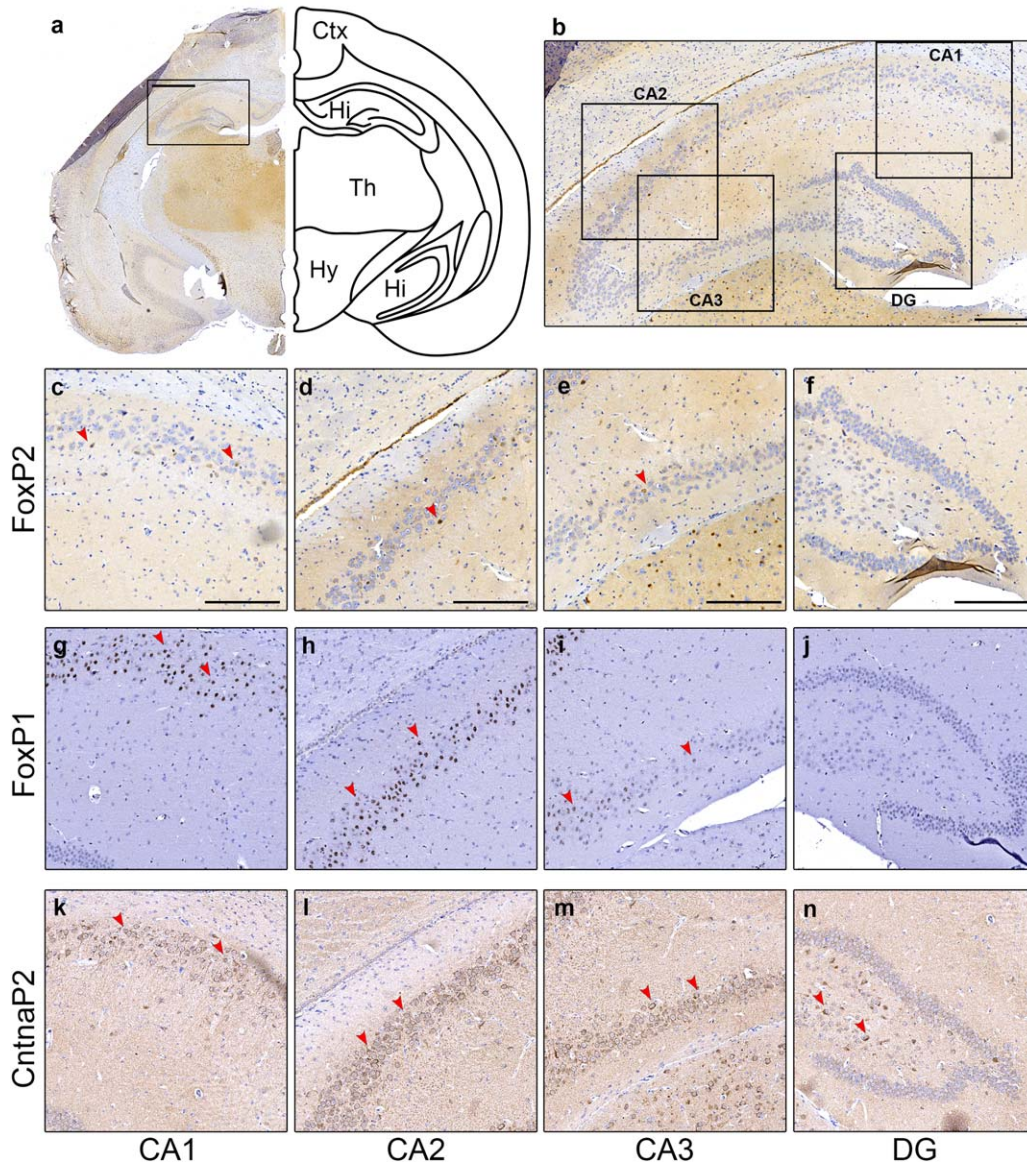
FIGURE 12 Distribution of FoxP2, FoxP1, and CntnaP2 in the hippocampus of *P. discolor*. Structural overview of the *P. discolor* brain slice (immunostained against FoxP2) used to select inset boxes, including simplified line diagrams indicating key brain regions represented (a). See Figure 3 for an indication of slice depth. Higher magnification of the hippocampus (b) shows further black inset boxes representing highest magnification insets detailing the CA1, CA2, CA3, and DG regions. FoxP2 shows little expression in the hippocampus besides rare neurons (c–f). FoxP1 is consistently expressed in CA1–3 (g–j) and CntnaP2 in CA1–3 and the DG (k–n). Scale bar in panel (a) represents 1 mm, panel (b) represents 250 μm, and scale bars in panel's (c–n) represent 200 μm. Brain structures are abbreviated as follows; Cortex (Ctx), Thalamus (Th), Hypothalamus (Hy) and hippocampus (Hi). Red arrows indicate examples of positively stained cells

et al., 2017). While FoxP2 expression was strong in *R. aegyptiacus* cortex, including the auditory and anterior cingulate cortical areas, only sparse FoxP2 staining could be observed in the adult *P. discolor* cortex. In *P. discolor* juveniles however, cortical staining was strongly enriched in deep layers of the primary auditory cortex and posterior dorsal field (PDF) of the auditory cortex, suggesting that FoxP2 could play a role in postnatal development of these brain regions. Of note, the PDF of the *P. discolor* auditory cortex contains combination sensitive neurons that form a chronotopic map of echo delay (Greiter & Firzlaff, 2017). In the mustached bat (*Pteronotus parnellii*), neurons in comparable regions of the auditory cortex are specialized for

processing communication calls (Ohlemiller, Kanwal, & Suga, 1996) and are sensitive to the combinations of, and temporal relationships between, syllables of these calls (Ohlemiller et al., 1996; Esser, Condon, Suga, & Kanwal, 1997). These data suggest there could be a specific role for neurons in this FoxP2 positive region of the auditory cortex in processing temporal and syntactical information embedded in communication calls of bats.

The auditory cortex makes strong reciprocal connections to the auditory thalamus (the ventral medial geniculate nucleus; vMGN), which can dynamically shape auditory representations (Radtke-Schuller, 2004). In other bat species the dorsal fields of the auditory cortex
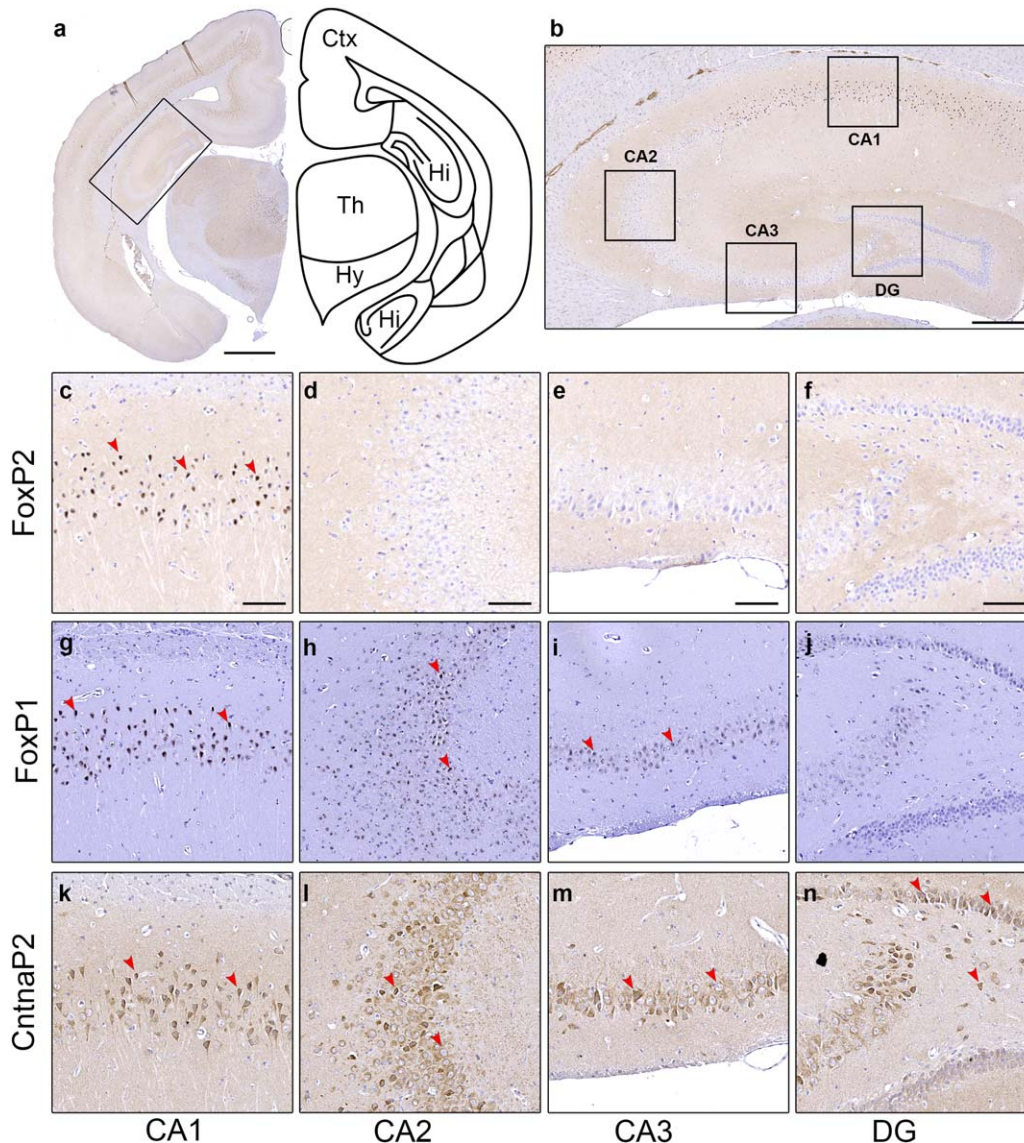
FIGURE 13 Distribution of FoxP2, FoxP1, and CntnaP2 in the hippocampus of *R. aegyptiacus*. Structural overview of the *P. discolor* brain slice (immunostained against FoxP2) used to create inset boxes, including simplified line diagrams indicating key brain regions represented (a). See Figure 3 for an indication of slice depth. Higher magnification of the hippocampus (b) shows further black inset boxes representing highest magnification insets detailing the CA1, CA2, CA3, and DG regions. FoxP2 is expressed in the CA1 region (c), but not in any other region of the hippocampus (d–f). FoxP1 is consistently expressed in CA1–3 (g–j) and CntnaP2 in CA1–3 and the DG (k–n). Scale bar in panel (a) represents 2 mm, panel (b) represents 500 μm, and scale bars in panels (c–n) represent 200 μm. Brain structures are abbreviated as follows; Cortex (Ctx), Thalamus (Th), Hypothalamus (Hy) and hippocampus (Hi). Red arrows indicate examples of positively stained cells

receive connections from the dorsal medial geniculate body (dMGB) (Radtke-Schuller, Schuller, & O'neill, 2004). The vMGN and auditory cortex have also been shown to be a major source of input to frontal motor cortex in the mustache bat (Kobler, Isbey, & Casseday, 1987) and for *C. perspicillata*, a species closely related to *P. discolor*, neurons responsive to acoustic stimulation have been found in the frontal cortex (Eiermann & Esser, 2000). FoxP2 was strongly and abundantly expressed in the vMGN in both species, whereas FoxP1 was absent. CntnaP2 was strong and abundant in this region in *P. discolor*, but not in *R. aegyptiacus*. Together this may suggest that of these three genes, only FoxP2 is required in the auditory thalamus of both species.

The amygdala is important for evaluating incoming acoustic information and modulating the appropriate behavioral response (Gadziola, Grimsley, Shanbhag, & Wenstrup, 2012). The lateral nucleus of the amygdala receives auditory information from the auditory cortex and vMGN and has direct connections back to the auditory cortex (Amaral & Price, 1984; LeDoux, Farb, & Romanski, 1991). In bats the lateral nucleus of the amygdala is important for discrimination of communication calls (Gadziola et al., 2012; Gadziola, Shanbhag, & Wenstrup, 2016). In the lateral nucleus of the amygdala of both species FoxP1 showed strong and abundant staining, while Foxp2 was largely absent. CntnaP2 was strong and abundant in *R. aegyptiacus* but weak and sparse in *P. discolor*. As
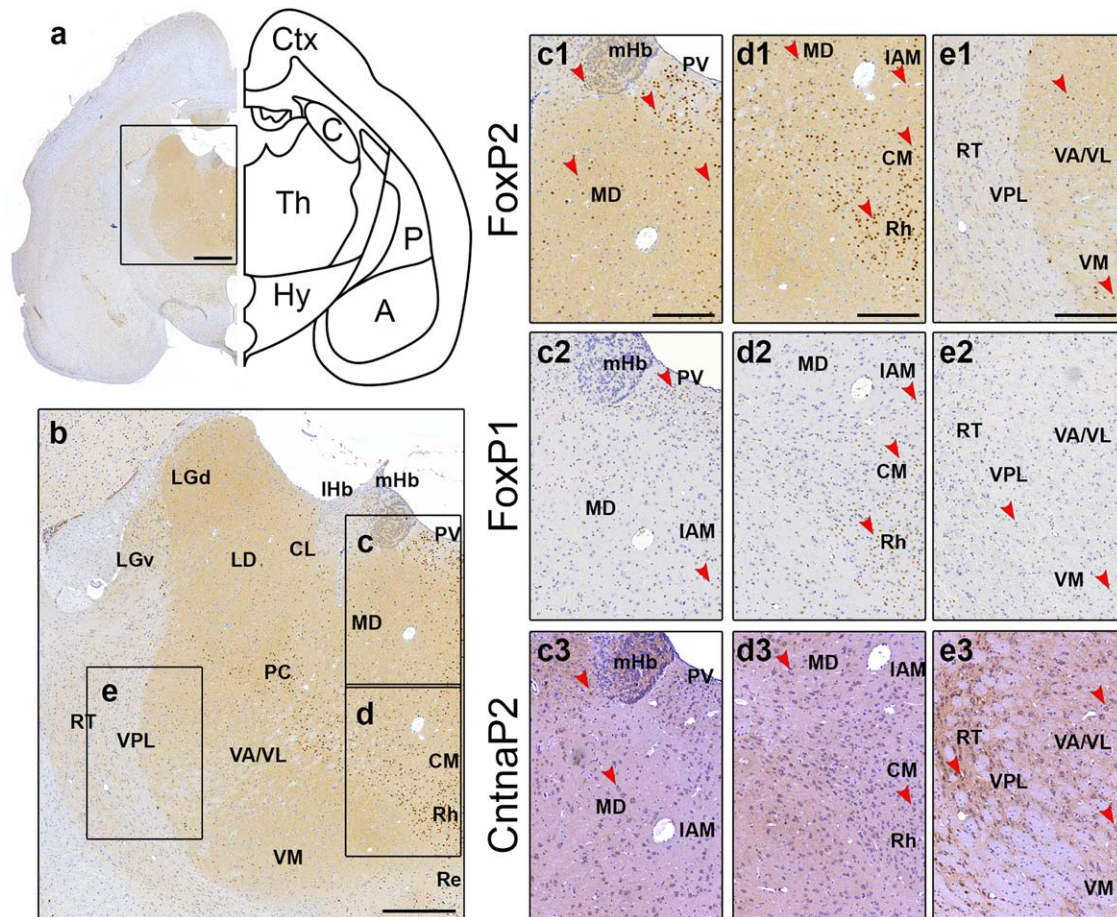
FIGURE 14 Distribution of FoxP2, FoxP1 and CntnaP2 in the thalamus of *P. discolor*. Structural overview of the *P. discolor* brain slice (immunostained against FoxP2) including simplified line diagrams indicating key brain regions (a), used to select inset boxes (b). See Figure 3 for an indication of slice depth. High magnification images display expression patterns of FoxP2 (c1, d1, e1), FoxP1 (c2, d2, e2) and CntnaP2 (c3, d3, e3). Scale bar in panel (a) represents 1 mm, panel (b) represents 500 μm, and scale bars in panels (c1–e3) can be found in (c1, b1, and c1) and represent 250 μm. Brain structures are abbreviated as follows: Cortex (Ctx), Caudate (C), Putamen (P), Thalamus (Th), Hypothalamus (Hy), Hippocampus (Hi) and Amygdala (A). Thalamic nuclei are abbreviated as follows: Centrolateral nucleus (CL), Centromedial nucleus (CM), Laterodorsal nucleus (LD), lateral Habenular nucleus (lHb), lateral Geniculate nucleus, dorsal (LGd), lateral Geniculate nucleus, ventral (LGv), Mediodorsal nucleus (MD), medial Habenular nucleus (mHb), Paracentral nucleus (PC), Paraventricular nucleus (PV), Rhomboidal nucleus (Rh), nucleus of Reuniens (Re), Reticular nucleus (RT), Ventral anterior nucleus (VA), Ventrolateral nucleus (VL), Ventromedial nucleus (VM) and Ventroposterolateral nucleus (VPL). Red arrows indicate examples of positively stained cells

such we see an inverse pattern to what was observed in the vMGN, with FoxP1 appearing to be most important of the three genes for the lateral nucleus of the amygdala in both species.

4.2 | Forebrain circuits relevant for vocal learning— vocal motor circuitry

FoxP2 has previously been observed to be strongly expressed throughout two cortical-subcortical loops controlling motor functions in mammals; the fronto-striatal and fronto-cerebellar circuits. This pattern of expression is largely conserved across rodents, non-human primates and the developing human brain, with only subtle differences observed across these highly evolutionarily distinct mammals (Ferland et al., 2003; Lai et al., 2003; Takahashi, Liu, Hirokawa, & Takahashi, 2003, 2008a; Takahashi et al., 2008b; Campbell et al., 2009; Hisaoka,

Nakamura, Senba, & Morikawa, 2010; Fujita & Sugihara, 2012; Kato et al., 2014). Because these circuits also underlie speech production, a crucial role for Foxp2 has been hypothesized in motor function and human speech (Vargha-Khadem, Gadian, Copp, & Mishkin, 2005). Humans with heterozygous disruptions of *FOXP2* display motor dysfunctions that are largely localized to the vocal-motor domain (Lai et al., 2001; Watkins, Dronkers, & Vargha-Khadem, 2002) with corresponding neuro-pathology in regions of the brain showing high FOXP2 expression, including the striatum (Lai et al., 2003).

In songbirds, FoxP2 is highly expressed in the song learning circuitry (which resembles the frontal–striatal circuitry of mammals). Genetic reduction of FoxP2 expression in a key component of this circuit known as area X (comparable to the mammalian striatum) resulted in juvenile animals that were less accurate at learning their songs, and adults that produced more variable song (Haesler et al., 2007;
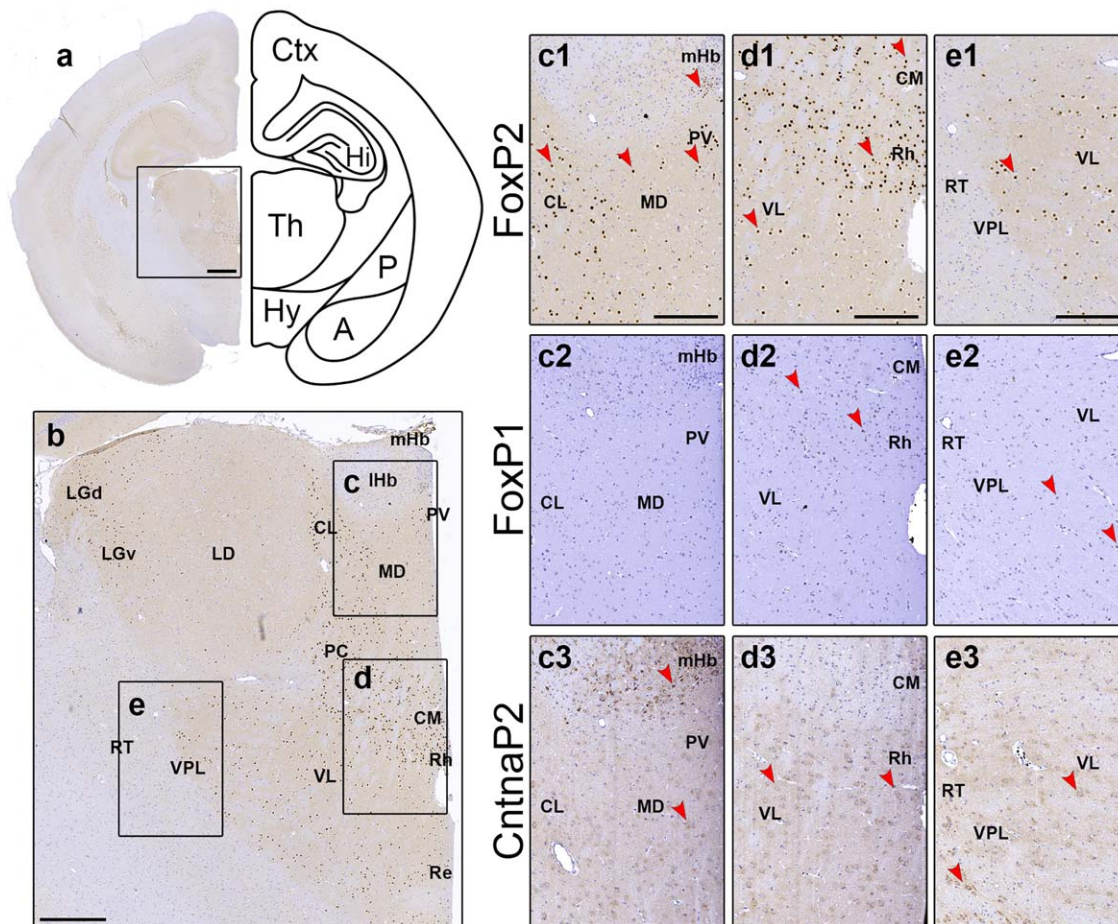
FIGURE 15 Distribution of FoxP2, FoxP1, and CntnaP2 in the thalamus of *R. aegyptiacus*. Structural overview of the *R. aegyptiacus* brain slice (immunostained against FoxP2) including simplified line diagrams indicating key brain regions (a), used to select inset boxes (b). See Figure 3 for an indication of slice depth. High magnification images display expression patterns of FoxP2 (c1, d1, e1), FoxP1 (c2, d2, e2) and CntnaP2 (c3, d3, e3). Scale bar in panel (a) represents 1 mm, panel (b) represents 500 μm, and scale bars in panels (c1–e3) can be found in (c1, b1, and c1) and represent 250 μm. Brain structures are abbreviated as follows: Cortex (Ctx), Caudate (C), Putamen (P), Thalamus (Th), Hypothalamus (Hy), Hippocampus (Hi) and Amygdala (A). Thalamic nuclei are abbreviated as follows: Centrolateral nucleus (CL), Centromedial nucleus (CM), Laterodorsal nucleus (LD), lateral Habenular nucleus (lHb), lateral Geniculate nucleus, dorsal (LGd), lateral Geniculate nucleus, ventral (LGv), Mediodorsal nucleus (MD), medial Habenular nucleus (mHb), Paracentral nucleus (PC), Paraventricular nucleus (PV), Rhomboidal nucleus (Rh), nucleus of Reuniens (Re), Reticular nucleus (RT), Ventral anterior nucleus (VA), Ventrolateral nucleus (VL), Ventromedial nucleus (VM) and Ventroposterolateral nucleus (VPL). Red arrows indicate examples of positively stained cells

Murugan, Harward, Scharff, & Mooney, 2013), pointing to a key role in songbird vocal learning. Mice with heterozygous Foxp2 mutations, matching those found in humans, show a specific deficit in motor learning and altered striatal plasticity (Groszer et al., 2008; French et al., 2011). Together these data from human, songbird and mouse suggest that pathways involving the striatum and contributing to motor learning, vocal learning and vocal-motor control are particularly sensitive to reductions in FoxP2 expression. Our data showed that FoxP2 is found in equivalent motor-related regions (cortico-striatal and cortico-cerebellar circuits—with the exception of the cortex in adult *P. discolor*) and strongly expressed in the striatum of both bats. Given the precise motor control needed for bat flight, their highly gregarious nature, and their reliance on vocalizations for both social interactions and navigation, we predict that FoxP2 expression in these circuits is likely to contribute to bat motor function and vocal control.

FOXP1 is involved in a range of neurodevelopmental phenotypes, including but not limited to speech and language. Children with *FOXP1* mutations display deficits including general motor delay, mild to moderate cognitive impairment, speech/language problems and autistic characteristics (Hamdan et al., 2010; Horn, 2011; O'Roak et al., 2011; Le Fevre et al., 2013; Lozano et al., 2015). FoxP1 and Foxp2 show highly overlapping patterns of expression and are known to function as dimers to co-regulate some genes (Ferland et al., 2003; Li et al., 2004; Teramitsu, 2004; Bacon & Rappold, 2012). As such this broader profile in affected individuals may be related to the wider distribution of FOXP1 in the cortex and subsequent effects on cortical circuit development and function when its expression is reduced. In rodent and primate studies, Foxp1 has a widespread pattern of expression, usually being found across layers 2–6 and this was also true for bat FoxP1
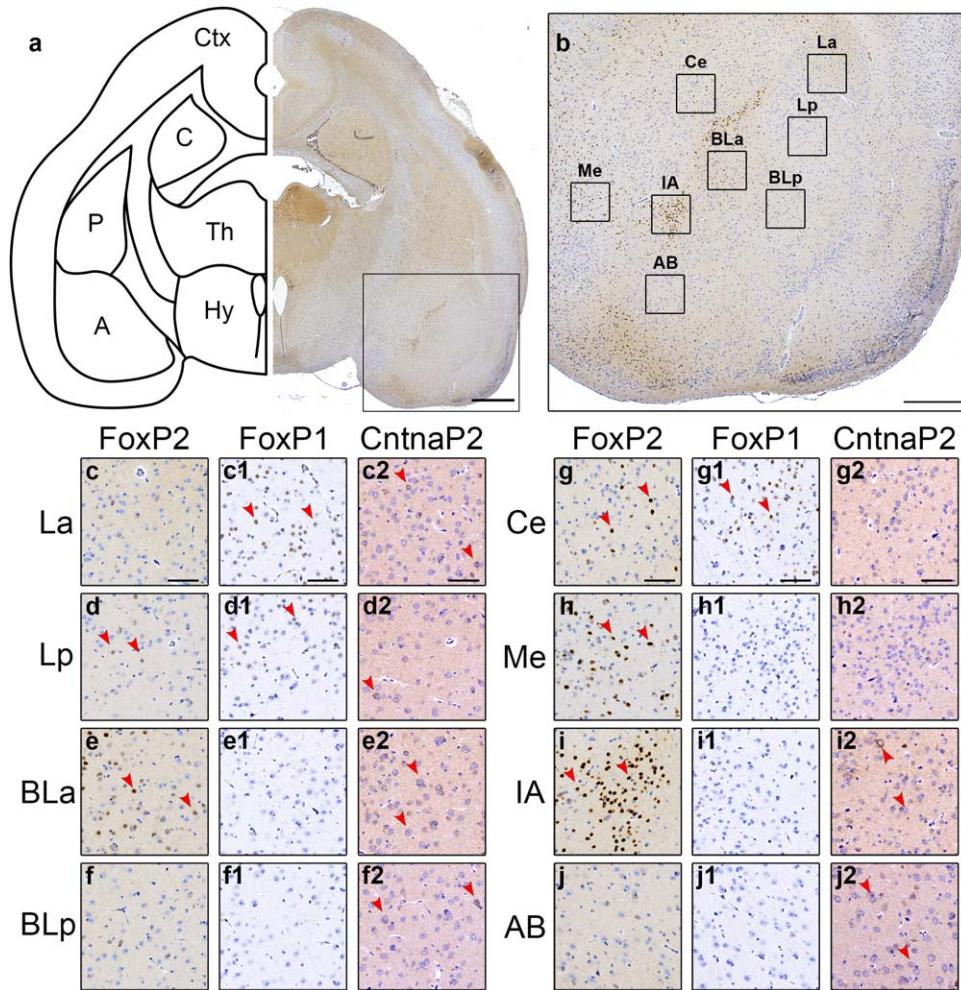
FIGURE 16 Distribution of FoxP2, FoxP1, and CntnaP2 in the amygdala of *P. discolor*. Structural overview of the *P. discolor* brain slice (immunostained against FoxP2) including simplified line diagrams indicating key brain regions used to select inset boxes (a). See Figure 3 for an indication of slice depth. Higher magnification image of the inset box (b) displays sub regions of the amygdala. Highest magnification images are shown for FoxP2 (c–j), FoxP1 (c1–j1) and CntnaP2 (c2–j2). Scale bar in panel (a) represents 1 mm, panel (b) represents 500 μm, and scale bars in panel's (c–j, c1–j1, c2–j2) represent 250 μm. Brain structures are abbreviated as follows; Lateral amygdaloid nucleus, pars anterior (La), Lateral amygdaloid nucleus, pars posterior (Lp), Basolateral amygdaloid nucleus, pars anterior (BLa), Basolateral amygdaloid nucleus, pars posterior (BLp), Central amygdaloid nucleus (Ce), Medial amygdaloid nucleus (Me), Intercalated amygdaloid nucleus (IA) and Accessory basal amygdaloid complex (AB). Red arrows indicate examples of positively stained cells

(Ferland et al., 2003; Hisaoka et al., 2010; Kato et al., 2014). Loss of Foxp1 in mice is embryonic lethal, however a brain specific knockout produced mice with behavioral impairments reflecting some of the human phenotypes including impaired short term memory, hyperactivity, increased repetitive behavior and reduced social interactions (Bacon et al., 2015). This was coupled with dramatic effects on striatal and hippocampal development, suggesting that loss of FoxP1 expression in these regions could also contribute to the phenotypes resulting from *FoxP1* mutations in both humans and mice. Both bat species showed abundant FoxP1 expression across layers 2–6 of the cortex and also showed strong and abundant expression in the striatum and the hippocampus. This expression pattern was highly overlapping in both species and matched closely with what has been observed in other mammals. This suggests that while FoxP1 is likely to play a role in bat vocal-motor and vocal

learning circuits, it is expected to have widespread effects beyond these circuits and may also contribute to general cognitive abilities and social interactions.

CNTNAP2 shows a complex but critical contribution to human neurodevelopment. Mutations in human *CNTNAP2* result in epilepsy, intellectual disability, autistic phenotypes, and speech/language impairments (Strauss et al., 2006; Jackman, Horn, Molleston, & Sokol, 2009; Gregor et al., 2011; O'Roak et al., 2011; Rodenas-Cuadrado et al., 2014; Rodenas-Cuadrado et al., 2016). Common variation in this gene has also been associated with language impairment, autism, and metrics of language development in the normal population (Alarcón et al., 2008; Arking et al., 2008; Bakkaloglu et al., 2008; Vernes et al., 2008; Peter et al., 2011; Whitehouse, Bishop, Ang, Pennell, & Fisher, 2011), suggesting that while complete disruption of this gene has severe and widespread effects on neurodevelopment, subtle variation in the gene
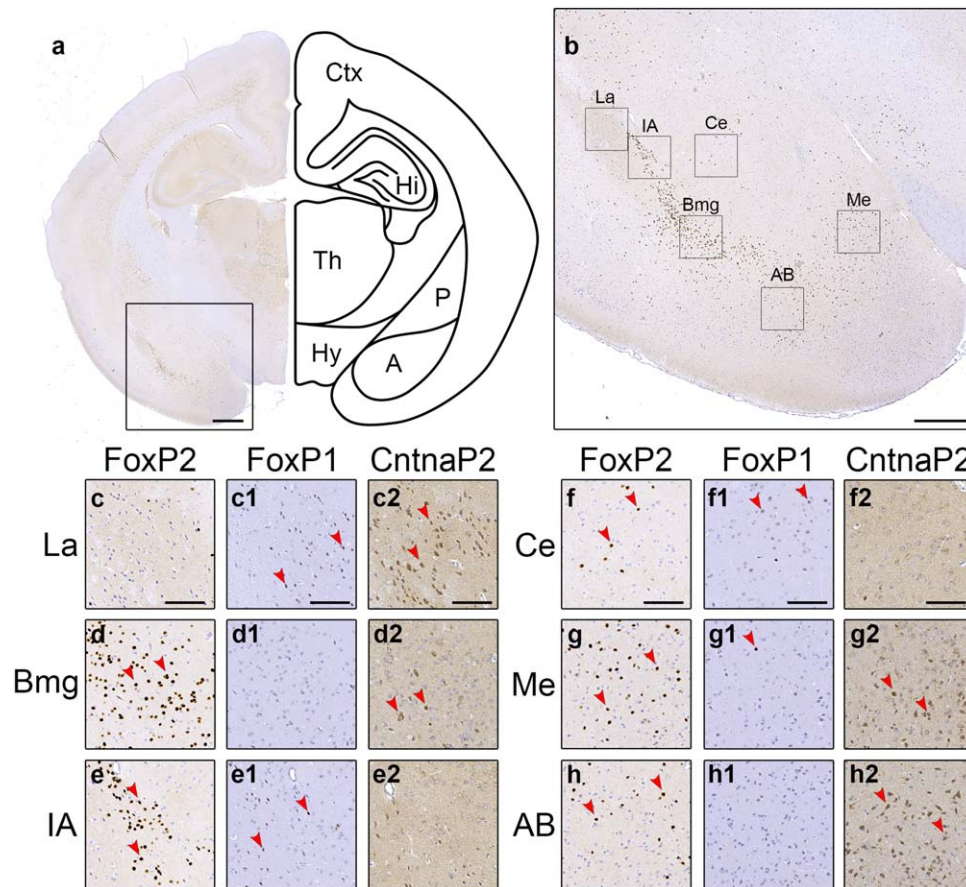
FIGURE 17 Distribution of FoxP2, FoxP1, and CntnaP2 in the amygdala of *R. aegyptiacus*. Structural overview of the *R. aegyptiacus* brain slice (immunostained against FoxP2) used to select inset boxes (a), including simplified line diagrams indicating key brain regions represented. See Figure 3 for an indication of slice depth. Higher magnification image of the inset box (b) displays sub regions of the amygdala. Highest magnification images are shown for FoxP2 (c–h), FoxP1 (c1–h1) and CntnaP2 (c2–h2). Scale bar in panel (a) represents 1 mm, panel (b) represents 500 μm, and scale bars in panel's (c–h, c1–h1, c2–h2) represent 250 μm. Brain structures are abbreviated as follows; Cortex (Ctx), Caudate (C), Putamen (P), Thalamus (Th), Hypothalamus (Hy) and Amygdala (A). Amygdala sub regions are abbreviated as follows: Lateral amygdaloid nucleus, pars anterior (La), Basal nucleus of the amygdala, magnocellular part (Bmg), Intercalated amygdaloid nucleus (IA), Central amygdaloid nucleus (Ce), Medial amygdaloid nucleus (Me), and Accessory basal amygdaloid complex (AB). Red arrows indicate examples of positively stained cells

could specifically affect speech, language, and social communication related circuits. Knockout mice lacking Cntnap2 had neuronal phenotypes like altered neuronal firing and seizures, but also displayed behavioral phenotypes including improved motor coordination, reduced social interactions, and increased repetitive behavior (Penagarikano et al., 2011). As for the other genes tested, we observed expression of CntnaP2 in multiple brain regions of both bats. In primate and rodent brains, CntnaP2 is strongly expressed in the cortex (layers 2–5), striatum and thalamus (Abrahams et al., 2007; Alarcón et al., 2008; Kato et al., 2014; Rodenas-Cuadrado et al., 2014). In the human brain, enrichment has been reported in the frontal cortex Broca's area and other perisylvian brain regions, suggesting an important role in development of higher order cognitive functions including speech and language (Abrahams et al., 2007). The expression pattern observed for CntnaP2 in these bats was similar to that seen in humans and rodents and expression of CntnaP2 often showed an inverse pattern to that of FoxP2. For example, Cntnap2 expression is very rare in the caudate–putamen, high in the globus pallidus and high in layer 5 of the cortex. FoxP2 was high in the caudate–putamen, very rare in the globus pallidus and highest in layer 6 of the cortex (except for the *P. discolor* cortex). Although their expression is not always mutually exclusive (for example both are expressed in the Purkinje cell layer of the cerebellum), the inverse expression pattern generally expressed by these proteins is consistent with the role of FOXP2 as a repressor of CNTNAP2 expression (Vernes et al., 2008).

Both CntnaP2 and FoxP1 remain strong candidates to contribute to bat vocal learning via their functions in the brain regions described above. In addition to this, their broader expression patterns and phenotypes caused by mutations (in comparison to FoxP2) means that they also represent candidates that could influence social behaviors. Given the extensive social groups in which bats live and their reliance on social (vocal) communication, they represent an interesting model to study the effects of these genes on the production of social vocalizations or social learning.
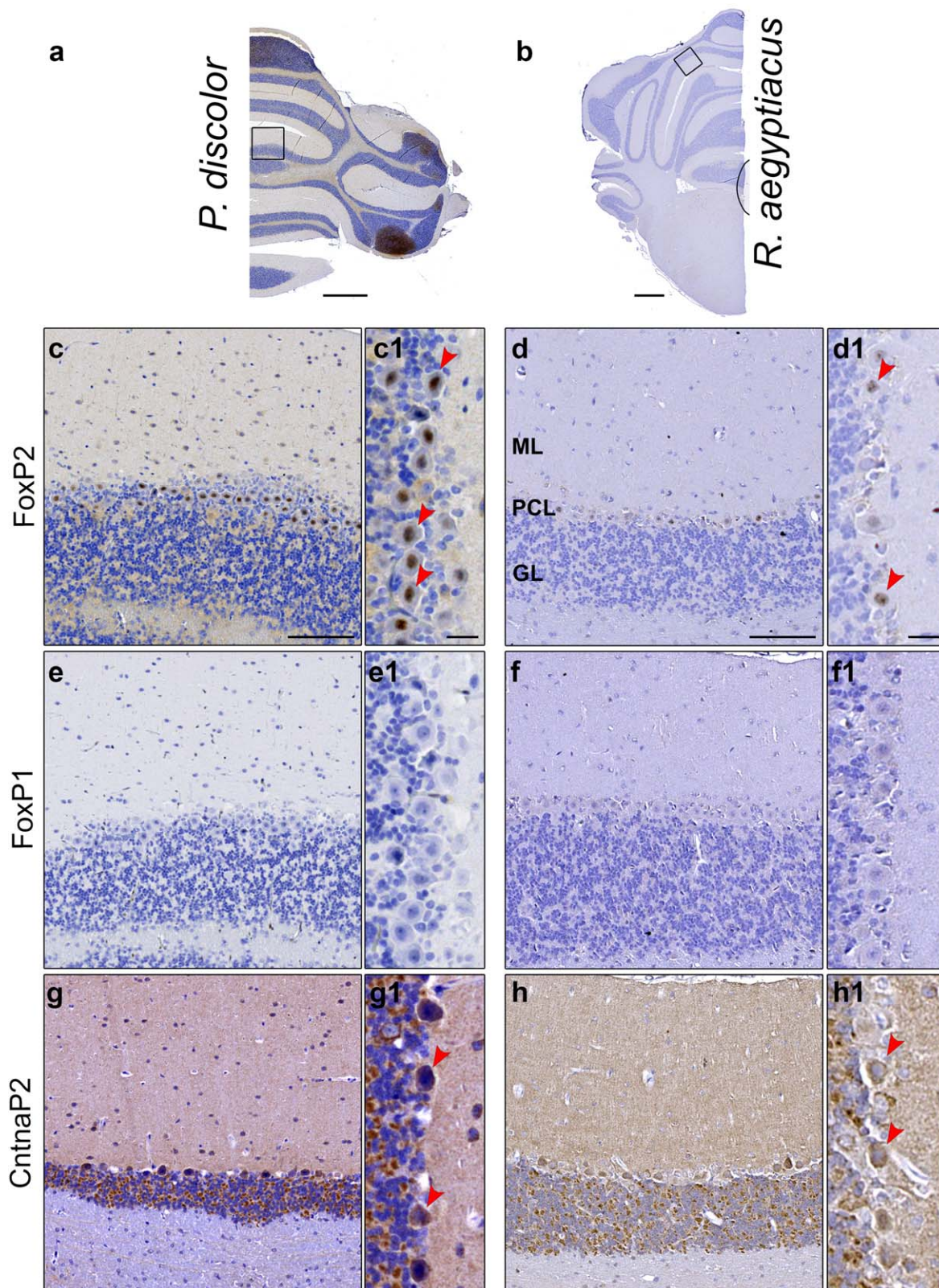
FIGURE 18 Distribution of FoxP2, FoxP1, and CntnaP2 in the cerebellum of *P. discolor* and *R. aegyptiacus*. Structural overview of the *P. discolor* (a) and *R. aegyptiacus* (b) brain slices (immunostained against FoxP2) used to create inset boxes. See Figure 3 for an indication of slice depth in each species. Inset images display that the expression patterns of FoxP2 (c, d), FoxP1 (e, f) and CntnaP2 (g, h) are highly conserved across species. High magnification images (c1–h1) were included to facilitate visualization of fine detail. Scale bar in panels (a, b) represent 1 mm, panels (c–h) represent 125 μm, and scale bars in panels (c1–h1) represent 20 μm. Brain structures are abbreviated as follows; ML = molecular layer, PCL = Purkinje cell layer, GL = granular layer and red arrows indicate examples of positively stained cells

4.3 | FoxP2 expression in the cortex shows a divergent pattern between the two bat species tested

FoxP2 has shown strong enrichment in deep layers of the cortex in all mammals (rodents and nonhuman primates) tested to date (Ferland et al., 2003; Lai et al., 2003; Campbell et al., 2009; Hisaoka et al., 2010; Kato et al., 2014). Little information is available for adult human brain, but in embryos, human FOXP2 is similarly restricted to deep layers of the developing cortex (Lai et al., 2003). Our study showed that this deep layer enrichment was found in adult *R. aegyptiacus*, but not in the adult *P. discolor* cortex.

The role of FoxP2 expression in the adult cortex is not well understood and in animal models, the requirement for FOXP2 in cortical neurons in adulthood has not yet been addressed. However the two bats investigated herein represent a naturally occurring "experiment" in that we have one species, *R. aegyptiacus*, with strong deep layer cortex FoxP2 expression and another, *P. discolor*, with very little FoxP2 in the adult cortex. Given that both these species are thought to be vocal learners, it follows that maintaining strong cortical FoxP2 expression into adulthood is not a universal feature of vocal learning animals. However, this broad conclusion should be tempered by the fact that we are still in the very early stages of understanding vocal learning in bats, the age at which it can occur, and the neural circuitry involved (Knornschild, 2014; Vernes, 2017). Importantly in both bat species the evidence for vocal learning comes from young animals (Esser, 1994; Prat et al., 2015) and until we determine if either species is capable of adult vocal learning, we can only speculate on the consequences of adult cortical FoxP2 expression in this process.

Interestingly *R. aegyptiacus* also showed enrichment of FoxP2 in layer 4 of the cortex, a property not shared with rodents or nonhuman primates (Campbell et al., 2009; Kato et al., 2014). While it would be possible to speculate on the function of this unusual layer 4 expression pattern in *R. aegyptiacus* bats, neurobehavioral work will be needed to determine if these neurons show altered properties or connectivity, or if the presence of FoxP2 in these neurons contributes to specific behaviors such as sensorimotor integration or vocal learning. In the future, functional, and neuro-behavioral studies, such as targeted knockdown experiments, will be critical for understanding the function of FoxP2 in vocal-motor control and/or vocal learning in the developing and adult cortex and could help explain the distinctive expression patterns we find in these two vocal learning species.

4.4 | Species specific differences in expression of FoxP2, FoxP1, and CntnaP2 across bats

In addition to the striking cortical expression difference observed across the two bat species, a few other differences in the distribution of FoxP2, FoxP1, and CntnaP2 were observed. In all animals tested to date FoxP2 has been largely absent from the hippocampus (Ferland et al., 2003; Lai et al., 2003; Takahashi et al., 2003, 2008a; Takahashi et al., 2008b; Campbell et al., 2009; Hisaoka et al., 2010; Fujita & Sugihara, 2012; Kato et al., 2014). This pattern was recapitulated in *P. discolor*, which displayed only some very rare, weak staining of cells in CA1–3. By contrast, FoxP2 was strongly and abundantly expressed in CA1 and the subiculum of the hippocampus of *R. aegyptiacus*. Given that CA1 is the major output pathway of the hippocampus and that place neurons have been identified in this region in *R. aegyptiacus* (Yartsev & Ulanovsky, 2013), this could reflect a role for FoxP2 in memory and/or navigation in this species however molecular and functional testing are crucial to test such hypotheses. Finally, small species specific differences were observed in the thalamus for all three genes. FoxP2 was expressed across much of the ventral nuclear group of *P. discolor* but absent from the equivalent region in *R. aegyptiacus*. In contrast, FoxP1 was more highly expressed in these nuclei in *R. aegyptiacus*. CntnaP2 was highly abundant in the geniculate group of thalamic nuclei in *P. discolor*, but absent in *R. aegyptiacus*. Cntnap2 was also highly expressed in a number of regions of the amygdala in *R. aegyptiacus*, but showed very little expression in *P. discolor*. Given that these are highly divergent species, these expression differences may reflect some of the phenotypic differences observed between these bats, however knock-out or knock-in experiments would be required to link expression patterns to functional outcomes.

5 | CONCLUSION

FOXP2, *FOXP1*, and *CNTNAP2* have been strongly implicated in the development and function of neural circuitry subserving human speech and language. We detailed the distribution of these proteins across the brains of two highly social and vocal learning bat species. We found expression patterns that broadly reflected those seen in humans and other mammals. A notable exception was the sparse expression of FoxP2 in the cortex of adult *P. discolor*, suggesting that adult Foxp2 expression in the cortex may not be a universal feature of vocal learning mammals. This work highlights brain regions that may be important for vocal-motor or vocal learning behavior in bats including areas of the auditory cortex, cingulate gyrus, basal ganglia, vMGN of the thalamus, and lateral nuclei of the amygdala, pinpointing these areas for further study. Functional neurogenetic studies in these species will be of great value to understand the role of these genes in vocal-motor and vocal learning behavior in mammals.

AUTHORS CONTRIBUTIONS

Study concept and design, and writing article: SCV. Sample acquisition: PMRC, TAS, MY, UF and SCV. Data acquisition and analysis of data: PMRC, JM, PD, LB and SCV. Critical revision of the article: JM, PD, MY, TAS, UF and SCV.

CONFLICT OF INTEREST

The authors declare that they have no conflict of interest

ORCID

Sonja C. Vernes http://orcid.org/0000-0003-0305-4584

REFERENCES

Abrahams, B. S., Tentler, D., Perederiy, J. V., Oldham, M. C., Coppola, G., & Geschwind, D. H. (2007). Genome-wide analyses of human perisylvian cerebral cortical patterning. *Proceedings of the National Academy of Sciences of the United States of America*, 104(45), 17849–17854.

Alarcón, M., Abrahams, B. S., Stone, J. L., Duvall, J. A., Perederiy, J. V., Bomar, J. M., ... Geschwind, D. H. (2008). Linkage, association, and gene-expression analyses identify CNTNAP2 as an autism-susceptibility gene. *American Journal of Human Genetics*, 82(1), 150–159.

Amaral, D. G., & Price, J. L. (1984). Amygdalo-cortical projections in the monkey (*Macaca fascicularis*). *The Journal of Comparative Neurology*, 230(4), 465–496.

Arking, D. E., Cutler, D. J., Brune, C. W., Teslovich, T. M., West, K., Ikeda, M., ... Chakravarti, A. (2008). A common genetic variant in the neurexin superfamily member CNTNAP2 increases familial risk of autism. *American Journal of Human Genetics*, 82(1), 160–164.

Bacon, C., & Rappold, G. A. (2012). The distinct and overlapping phenotypic spectra of FOXP1 and FOXP2 in cognitive disorders. *Human Genetics*, 131(11), 1687–1698.

Bacon, C., Schneider, M., Le Magueresse, C., Froehlich, H., Sticht, C., Gluch, C., ... Rappold, G. A. (2015). Brain-specific Foxp1 deletion impairs neuronal development and causes autistic-like behaviour. *Molecular Psychiatry*, 20(5), 632–639.

Bakkaloglu, B., O'roak, B. J., Louvi, A., Gupta, A. R., Abelson, J. F., Morgan, T. M., ... State, M. W. (2008). Molecular cytogenetic analysis and resequencing of contactin associated protein-like 2 in autism spectrum disorders. *American Journal of Human Genetics*, 82(1), 165–173.

Baron, G., Stephan, H., & Frahm, H. D. (1996). *Comparative neurobiology in Chiroptera*. Basel: Birkhäuser Verlag.

Bolhuis, J. J., Okanoya, K., & Scharff, C. (2010). Twitter evolution: Converging mechanisms in birdsong and human speech. *Nature Reviews. Neuroscience*, 11(11), 747–759.

Brainard, M. S., & Doupe, A. J. (2000). Auditory feedback in learning and maintenance of vocal behaviour. *Nature Reviews. Neuroscience*, 1(1), 31–40.

Brainard, M. S., & Doupe, A. J. (2013). Translating birdsong: Songbirds as a model for basic and applied medical research. *Annual Review of Neuroscience*, 36, 489–517.

Campbell, P., Reep, R. L., Stoll, M. L., Ophir, A. G., & Phelps, S. M. (2009). Conservation and diversity of Foxp2 expression in muroid rodents: Functional implications. *The Journal of Comparative Neurology*, 512(1), 84–100.

Condro, M. C., & White, S. A. (2014). Distribution of language-related Cntnap2 protein in neural circuits critical for vocal learning. *The Journal of Comparative Neurology*, 522(1), 169–185.

Dear, S. P., Fritz, J., Haresign, T., Ferragamo, M., & Simmons, J. A. (1993). Tonotopic and functional organization in the auditory cortex of the big brown bat, *Eptesicus fuscus*. *Journal of Neurophysiology*, 70(5), 1988–2009.

Doupe, A. J., & Kuhl, P. K. (1999). Birdsong and human speech: Common themes and mechanisms. *Annual Review of Neuroscience*, 22, 567–631.

Doupe, A. J., Perkel, D. J., Reiner, A., & Stern, E. A. (2005). Birdbrains could teach basal ganglia research a new song. *Trends in Neurosciences*, 28(7), 353–363.

Doupe, A. J., Solis, M. M., Kimpo, R., & Boettiger, C. A. (2004). Cellular, circuit, and synaptic mechanisms in song learning. *Annals of the New York Academy of Sciences*, 1016, 495–523.

Ehret, G. (1997). The auditory cortex. *Journal of Comparative Physiology. A, Sensory, Neural, and Behavioral Physiology*, 181(6), 547–557.

Eiermann, A., & Esser, K. H. (2000). Auditory responses from the frontal cortex in the short-tailed fruit bat *Carollia perspicillata*. *Neuroreport*, 11(2), 421–425.

Esser, K. H. (1994). Audio-vocal learning in a non-human mammal: The lesser spear-nosed bat Phyllostomus discolor. *Neuroreport*, 5(14), 1718–1720.

Esser, K. H., Condon, C. J., Suga, N., & Kanwal, J. S. (1997). Syntax processing by auditory cortical neurons in the FM-FM area of the mustached bat *Pteronotus parnellii*. *Proceedings of the National Academy of Sciences of the United States of America*, 94(25), 14019–14024.

Esser, K. H., & Eiermann, A. (1999). Tonotopic organization and parcellation of auditory cortex in the FM-bat *Carollia perspicillata*. *The European Journal of Neuroscience*, 11(10), 3669–3682.

Esser, K. H., & Kiefer, R. (1996). Detection of frequency modulation in the FM-bat Phyllostomus discolor. *Journal of Comparative Physiology. A, Sensory, Neural, and Behavioral Physiology*, 178(6), 787–796.

Esser, K. H., & Schmidt, U. (1989). Mother-infant communication in the lesser spear-nosed bat Phyllostomus-discolor (Chiroptera, Phyllostomidae) - evidence for acoustic learning. *Ethology*, 82(2), 156–168.

Esser, K. H., & Schmidt, U. (1990). Behavioral auditory thresholds in neonate lesser spear-nosed bats, Phyllostomus discolor. *Die Naturwissenschaften*, 77(6), 292–294.

Ferland, R. J., Cherry, T. J., Preware, P. O., Morrisey, E. E., & Walsh, C. A. (2003). Characterization of Foxp2 and Foxp1 mRNA and protein in the developing and mature brain. *The Journal of Comparative Neurology*, 460(2), 266–279.

Fisher, S. E., & Scharff, C. (2009). FOXP2 as a molecular window into speech and language. *Trends in Genetics: TIG*, 25(4), 166–177.

French, C. A., Jin, X., Campbell, T. G., Gerfen, E., Groszer, M., Fisher, S. E., & Costa, R. M. (2011). An aetiological Foxp2 mutation causes aberrant striatal activity and alters plasticity during skill learning. *Molecular Psychiatry*, 17(11), 1077–1085.

Fujita, H., & Sugihara, I. (2012). FoxP2 expression in the cerebellum and inferior olive: Development of the transverse stripe-shaped expression pattern in the mouse cerebellar cortex. *The Journal of Comparative Neurology*, 520(3), 656–677.

Gadziola, M. A., Grimsley, J. M., Shanbhag, S. J., & Wenstrup, J. J. (2012). A novel coding mechanism for social vocalizations in the lateral amygdala. *Journal of Neurophysiology*, 107(4), 1047–1057.

Gadziola, M. A., Shanbhag, S. J., & Wenstrup, J. J. (2016). Two distinct representations of social vocalizations in the basolateral amygdala. *Journal of Neurophysiology*, 115(2), 868–886.

Goldstein, M. H., King, A. P., & West, M. J. (2003). Social interaction shapes babbling: Testing parallels between birdsong and speech. *Proceedings of the National Academy of Sciences of the United States of America*, 100(13), 8030–8035.

Gordon, A., Salomon, D., Barak, N., Pen, Y., Tsoory, M., Kimchi, T., & Peles, E. (2016). Expression of Cntnap2 (Caspr2) in multiple levels of sensory systems. *Molecular and Cellular Neurosciences*, 70, 42–53.

Gregor, A., Albrecht, B., Bader, I., Bijlsma, E. K., Ekici, A. B., Engels, H., ... Zweier, C. (2011). Expanding the clinical spectrum associated with defects in CNTNAP2 and NRXN1. *BMC Medical Genetics*, 12, 106.

Greiter, W., & Firzlaff, U. (2017). Echo-acoustic flow shapes object representation in spatially complex acoustic scenes. *Journal of Neurophysiology, 117*(6), 2113–2124.

Groszer, M., Keays, D. A., Deacon, R. M., de Bono, J. P., Prasad-Mulcare, S., Gaub, S., ... Fisher, S. E. (2008). Impaired synaptic plasticity and motor learning in mice with a point mutation implicated in human speech deficits. *Current Biology: CB, 18*(5), 354–362.

Haesler, S., Rochefort, C., Georgi, B., Licznerski, P., Osten, P., & Scharff, C. (2007). Incomplete and inaccurate vocal imitation after knockdown of FoxP2 in songbird basal ganglia nucleus Area X. *PLoS Biology, 5* (12), e321.

Haesler, S., Wada, K., Nshdejan, A., Morrisey, E. E., Lints, T., Jarvis, E. D., & Scharff, C. (2004). FoxP2 expression in avian vocal learners and non-learners. *The Journal of Neuroscience: The Official Journal of the Society for Neuroscience, 24*(13), 3164–3175.

Hamdan, F. F., Daoud, H., Rochefort, D., Piton, A., Gauthier, J., Langlois, M., ... Michaud, J. L. (2010). De novo mutations in FOXP1 in cases with intellectual disability, autism, and language impairment. *American Journal of Human Genetics, 87*(5), 671–678.

Hevner, R. F. (2007). Layer-specific markers as probes for neuron type identity in human neocortex and malformations of cortical development. *Journal of Neuropathology and Experimental Neurology, 66*(2), 101–109.

Hilliard, A. T., Miller, J. E., Fraley, E. R., Horvath, S., & White, S. A. (2012). Molecular microcircuitry underlies functional specification in a basal ganglia circuit dedicated to vocal learning. *Neuron, 73*(3), 537–552.

Hisaoka, T., Nakamura, Y., Senba, E., & Morikawa, Y. (2010). The forkhead transcription factors, Foxp1 and Foxp2, identify different subpopulations of projection neurons in the mouse cerebral cortex. *Neuroscience, 166*(2), 551–563.

Hoffmann, S., Firzlaff, U., Radtke-Schuller, S., Schwellnus, B., & Schuller, G. (2008). The auditory cortex of the bat Phyllostomus discolor: Localization and organization of basic response properties. *BMC Neuroscience, 9*, 65.

Horn, D. (2011). Mild to moderate intellectual disability and significant speech and language deficits in patients with FOXP1 deletions and mutations. *Molecular Syndromology, 2*, 213–216.

Jabaudon, D., Shnider, S. J., Tischfield, D. J., Galazo, M. J., & Macklis, J. D. (2012). RORbeta induces barrel-like neuronal clusters in the developing neocortex. *Cerebral Cortex (New York, N.Y.: 1991), 22*(5), 996–1006.

Jackman, C., Horn, N. D., Molleston, J. P., & Sokol, D. K. (2009). Gene associated with seizures, autism, and hepatomegaly in an Amish girl. *Pediatric Neurology, 40*(4), 310–313.

Janik, V. M., & Slater, P. J. (2000). The different roles of social learning in vocal communication. *Animal Behaviour, 60*(1), 1–11.

Janik, V. M., & Slater, P. J. B. (1997). Vocal learning in mammals. *Advances in the Study of Behavior, 26*, 59–99.

Jarvis, E. D. (2004). Learned birdsong and the neurobiology of human language. *Annals of the New York Academy of Sciences, 1016*, 749–777.

Jarvis, E. D. (2007). Neural systems for vocal learning in birds and humans: A synopsis. *Journal of Ornithology, 148*(1), 35–44.

Jurgens, U. (2002). A study of the central control of vocalization using the squirrel monkey. *Medical Engineering & Physics, 24*(7–8), 473–477.

Jurgens, U. (2009). The neural control of vocalization in mammals: A review. *Journal of Voice, 23*(1), 1–10.

Kato, M., Okanoya, K., Koike, T., Sasaki, E., Okano, H., Watanabe, S., & Iriki, A. (2014). Human speech- and reading-related genes display partially overlapping expression patterns in the marmoset brain. *Brain and Language, 133*, 26–38.

Knornschild, M. (2014). Vocal production learning in bats. *Current Opinion in Neurobiology, 28C*, 80–85.

Kobler, J. B., Isbey, S. F., & Casseday, J. H. (1987). Auditory pathways to the frontal cortex of the mustache bat, *Pteronotus parnellii*. *Science (New York, N.Y.), 236*(4803), 824–826.

Lai, C. S., Fisher, S. E., Hurst, J. A., Vargha-Khadem, F., & Monaco, A. P. (2001). A forkhead-domain gene is mutated in a severe speech and language disorder. *Nature, 413*(6855), 519–523.

Lai, C. S., Gerrelli, D., Monaco, A. P., Fisher, S. E., & Copp, A. J. (2003). FOXP2 expression during brain development coincides with adult sites of pathology in a severe speech and language disorder. *Brain, 126*(Pt 11), 2455–2462.

Le Fevre, A. K., Taylor, S., Malek, N. H., Horn, D., Carr, C. W., Abdul-Rahman, O. A., ... Hunter, M. F. (2013). FOXP1 mutations cause intellectual disability and a recognizable phenotype. *American Journal of Medical Genetics Part A, 161A*(12), 3166–3175.

LeDoux, J. E., Farb, C. R., & Romanski, L. M. (1991). Overlapping projections to the amygdala and striatum from auditory processing areas of the thalamus and cortex. *Neuroscience Letters, 134*(1), 139–144.

Lein, E. S., Hawrylycz, M. J., Ao, N., Ayres, M., Bensinger, A., Bernard, A., ... Jones, A. R. (2007). Genome-wide atlas of gene expression in the adult mouse brain. *Nature, 445*(7124), 168–176.

Li, S., Weidenfeld, J., & Morrisey, E. E. (2004). Transcriptional and DNA binding activity of the Foxp1/2/4 family is modulated by heterotypic and homotypic protein interactions. *Molecular and Cellular Biology, 24* (2), 809–822.

Loh, K. K., Petrides, M., Hopkins, W. D., Procyk, E., & Amiez, C. (2016). Cognitive control of vocalizations in the primate ventrolateral-dorsomedial frontal (VLF-DMF) brain network. *Neuroscience & Biobehavioral Reviews, 82*, 32–44.

Lozano, R., Vino, A., Lozano, C., Fisher, S. E., & Deriziotis, P. (2015). A de novo FOXP1 variant in a patient with autism, intellectual disability and severe speech and language impairment. *European Journal of Human Genetics: EJHG, 23*(12), 1702–1707.

Mello, C. V. (2002). Mapping vocal communication pathways in birds with inducible gene expression. *Journal of Comparative Physiology. A, Neuroethology, Sensory, Neural, and Behavioral Physiology, 188*(11–12), 943–959.

Mooney, R. (2009). Neural mechanisms for learned birdsong. *Learning & Memory (Cold Spring Harbor, N.Y.), 16*(11), 655–669.

Morgan, A., Fisher, S., Scheffer, I., & Hildebrand, M. (2016). FOXP2-related speech and language disorders. GeneReviews® https://www.ncbi.nlm.nih.gov/books/NBK368474/

Moroni, R. F., Inverardi, F., Regondi, M. C., Watakabe, A., Yamamori, T., Spreafico, R., & Frassoni, C. (2009). Expression of layer-specific markers in the adult neocortex of BCNU-treated rat, a model of cortical dysplasia. *Neuroscience, 159*(2), 682–691.

Murugan, M., Harward, S., Scharff, C., & Mooney, R. (2013). Diminished FoxP2 levels affect dopaminergic modulation of corticostriatal signaling important to song variability. *Neuron, 80*(6), 1464–1476.

Nakagawa, J. M., Donkels, C., Fauser, S., Schulze-Bonhage, A., Prinz, M., Zentner, J., & Haas, C. A. (2017). Characterization of focal cortical dysplasia with balloon cells by layer-specific markers: Evidence for differential vulnerability of interneurons. *Epilepsia, 58*(4), 635–645.

O'Roak, B. J., Deriziotis, P., Lee, C., Vives, L., Schwartz, J. J., Girirajan, S., ... Eichler, E. E. (2011). Exome sequencing in sporadic autism spectrum disorders identifies severe de novo mutations. *Nature Genetics, 43*(6), 585–589.

Ohlemiller, K. K., Kanwal, J. S., & Suga, N. (1996). Facilitative responses to species-specific calls in cortical FM-FM neurons of the mustached bat. *Neuroreport, 7*(11), 1749–1755.

Panaitof, S. C., Abrahams, B. S., Dong, H., Geschwind, D. H., & White, S. A. (2010). Language-related Cntnap2 gene is differentially expressed in sexually dimorphic song nuclei essential for vocal learning in songbirds. *The Journal of Comparative Neurology*, *518*(11), 1995–2018.

Penagarikano, O., Abrahams, B. S., Herman, E. I., Winden, K. D., Gdalyahu, A., Dong, H., ... Geschwind, D. H. (2011). Absence of CNTNAP2 leads to epilepsy, neuronal migration abnormalities, and core autism-related deficits. *Cell*, *147*(1), 235–246.

Peter, B., Raskind, W. H., Matsushita, M., Lisowski, M., Vu, T., Berninger, V. W., ... Brkanac, Z. (2011). Replication of CNTNAP2 association with nonword repetition and support for FOXP2 association with timed reading and motor activities in a dyslexia family sample. *Journal of Neurodevelopmental Disorders*, *3*(1), 39–49.

Petkov, C. I., & Jarvis, E. D. (2012). Birds, primates, and spoken language origins: Behavioral phenotypes and neurobiological substrates. *Frontiers in Evolutionary Neuroscience*, *4*, 12.

Prat, Y., Taub, M., & Yovel, Y. (2015). Vocal learning in a social mammal: Demonstrated by isolation and playback experiments in bats. *Science Advances*, *1*(2), e1500019.

Radtke-Schuller, S. (2004). Cytoarchitecture of the medial geniculate body and thalamic projections to the auditory cortex in the rufous horseshoe bat (*Rhinolophus rouxi*). I. Temporal fields. *Anatomy and Embryology*, *209*(1), 59–76.

Radtke-Schuller, S., Schuller, G., & O'neill, W. E. (2004). Thalamic projections to the auditory cortex in the rufous horseshoe bat (Rhinolophus rouxi). II. Dorsal fields. *Anatomy and Embryology*, *209*(1), 77–91.

Rauschecker, J. P. (1998). Cortical processing of complex sounds. *Current Opinion in Neurobiology*, *8*(4), 516–521.

Roberts, T. F., Hisey, E., Tanaka, M., Kearney, M. G., Chattree, G., Yang, C. F., ... Mooney, R. (2017). Identification of a motor-to-auditory pathway important for vocal learning. *Nature Neuroscience*, *20*, 978–986.

Rodenas-Cuadrado, P., Ho, J., & Vernes, S. C. (2014). Shining a light on CNTNAP2: Complex functions to complex disorders. *European Journal of Human Genetics: EJHG*, *22*(2), 171–178.

Rodenas-Cuadrado, P., Pietrafusa, N., Francavilla, T., La Neve, A., Striano, P., & Vernes, S. C. (2016). Characterisation of CASPR2 deficiency disorder - A syndrome involving autism, epilepsy and language impairment. *BMC Medical Genetics*, *17*(1), 8.

Scalia, F. (2013). *Forebrain atlas of the short-tailed fruit bat, Carollia perpicillata: Prepared by the methods of Nissl and Neun immunohistochemistry*. New York, NY: Springer.

Scharff, C., & White, S. A. (2004). Genetic components of vocal learning. *Annals of the New York Academy of Sciences*, *1016*, 325–347.

Schneider, R. (1966). Das Gehirn von *Rousettus aegyptiacus* (E. Geoffroy 1810) (Megachiroptera, Chiroptera, Mammalia). Ein Mit Hilfe Mehrerer Schnittserien Erstellter Atlas. *Abhandlungen Der Senckenbergischen Naturforschenden Gesellschaft*, *513*, 1–160.

Sollis, E., Graham, S. A., Vino, A., Froehlich, H., Vreeburg, M., Dimitropoulou, D., ... Fisher, S. E. (2016). Identification and functional characterization of de novo FOXP1 variants provides novel insights into the etiology of neurodevelopmental disorder. *Human Molecular Genetics*, *25*(3), 546–557.

Strauss, K. A., Puffenberger, E. G., Huentelman, M. J., Gottlieb, S., Dobrin, S. E., Parod, J. M., ... Morton, D. H. (2006). Recessive symptomatic focal epilepsy and mutant contactin-associated protein-like 2. *The New England Journal of Medicine*, *354*(13), 1370–1377.

Takahashi, K., Liu, F. C., Hirokawa, K., & Takahashi, H. (2003). Expression of Foxp2, a gene involved in speech and language, in the developing and adult striatum. *Journal of Neuroscience Research*, *73*(1), 61–72.

Takahashi, K., Liu, F. C., Hirokawa, K., & Takahashi, H. (2008a). Expression of Foxp4 in the developing and adult rat forebrain. *Journal of Neuroscience Research*, *86*(14), 3106–3116.

Takahashi, K., Liu, F. C., Oishi, T., Mori, T., Higo, N., Hayashi, M., ... Takahashi, H. (2008b). Expression of FOXP2 in the developing monkey forebrain: Comparison with the expression of the genes FOXP1, PBX3, and MEIS2. *The Journal of Comparative Neurology*, *509*(2), 180–189.

Tanimoto, H., Teramitsu, I., Poopatanapong, A., Torrisi, S., & White, S. A. (2010). Striatal FoxP2 is actively regulated during songbird sensorimotor learning. *PLoS One*, *5*(1), e8548.

Teeling, E. C., Springer, M. S., Madsen, O., Bates, P., O'brien, S. J., & Murphy, W. J. (2005). A molecular phylogeny for bats illuminates biogeography and the fossil record. *Science (New York, N.Y.)*, *307*(5709), 580–584.

Teramitsu, I. (2004). Parallel FoxP1 and FoxP2 expression in songbird and human brain predicts functional interaction. *The Journal of Neuroscience*, *24*(13), 3152–3163.

Teramitsu, I. (2006). FoxP2 regulation during undirected singing in adult songbirds. *The Journal of Neuroscience*, *26*(28), 7390–7394.

Thompson, C. K., Schwabe, F., Schoof, A., Mendoza, E., Gampe, J., Rochefort, C., & Scharff, C. (2013). Young and intense: FoxP2 immunoreactivity in Area X varies with age, song stereotypy, and singing in male zebra finches. *Frontiers in Neural Circuits*, *7*, 24.

Ulanovsky, N., & Moss, C. F. (2008). What the bat's voice tells the bat's brain. *Proceedings of the National Academy of Sciences of the United States of America*, *105*(25), 8491–8498.

Vargha-Khadem, F., Gadian, D. G., Copp, A., & Mishkin, M. (2005). FOXP2 and the neuroanatomy of speech and language. *Nature Reviews. Neuroscience*, *6*(2), 131–138.

Vernes, S. C. (2017). What bats have to say about speech and language. *Psychonomic Bulletin & Review*, *24*(1), 111–117.

Vernes, S. C., Newbury, D. F., Abrahams, B. S., Winchester, L., Nicod, J., Groszer, M., ... Fisher, S. E. (2008). A functional genetic link between distinct developmental language disorders. *The New England Journal of Medicine*, *359*(22), 2337–2345.

Watkins, K. E., Dronkers, N. F., & Vargha-Khadem, F. (2002). Behavioural analysis of an inherited speech and language disorder: Comparison with acquired aphasia. *Brain*, *125*(Pt 3), 452–464.

White, S. A., Fisher, S. E., Geschwind, D. H., Scharff, C., & Holy, T. E. (2006). Singing mice, songbirds, and more: Models for FOXP2 function and dysfunction in human speech and language. *The Journal of Neuroscience*, *26*(41), 10376–10379.

Whitehouse, A. J., Bishop, D. V., Ang, Q. W., Pennell, C. E., & Fisher, S. E. (2011). CNTNAP2 variants affect early language development in the general population. *Genes, Brain, and Behavior*, *10*(4), 451–456.

Yartsev, M. M., & Ulanovsky, N. (2013). Representation of three-dimensional space in the hippocampus of flying bats. *Science (New York, N.Y.)*, *340*(6130), 367–372.

Yovel, Y., Geva-Sagiv, M., & Ulanovsky, N. (2011). Click-based echolocation in bats: Not so primitive after all. *Journal of Comparative Physiology. A, Neuroethology, Sensory, Neural, and Behavioral Physiology*, *197*(5), 515–530.